BTA/PE/12-01 **Title: Effect of Diffusion on Foam Bubble Size Distribution and Gas Mobility: an Idealized 2D Model**

Date 2012-01-12 **Student name: L.E. Nonnekes**

TU Delft

Department of Geotechnology

Delft University of Technology

Title	:	Effect of Diffusion on Foam bubble Size Distribution and Gas Mobility: an Idealized 2D model
Author(s)	:	L.E. Nonnekes
Date	:	2012-01-12
Professor(s)	:	Prof. W.R. Rossen
Supervisor(s)	:	Prof. W.R. Rossen
TA Report number	:	BTA/PE/12-01

Postal Address : Section for Petroleum Engineering
Department of Applied Earth Sciences
Delft University of Technology
P.O. Box 5028
The Netherlands
Telephone : (31) 15 2781328 (secretary)
Telefax : (31) 15 2781189

Abstract

In this thesis the effect of gas diffusion between bubbles on the bubble-size distribution and capillary resistance to foam flow in a bubble train is investigated using an idealized 2D pore model. First the shape of the model pore is discussed and how a lamella moves through it. Then the physical forces (lamella curvatures and pressure differences between bubbles) in the pores are explained and how they affect capillary resistance to foam flow. Next the parameters of the dimensionless model are related to measured fluid properties. Under certain conditions (large film permeability to gas, large surface tension, low pressure, small pores, and low velocity of flowing gas) it is possible that characteristic diffusion rate can be greater than imposed convection rate, and that all gas transport is from diffusion across lamellae, not bubble movement.

We present model results for different ratios of characteristic diffusion to convection rates. If bubbles are smaller than pores, diffusion reduces the number of bubbles and increases average bubble size, whether convection is imposed on the foam or not. If convection is imposed, lamellae disappear not in pore throats but after first colliding in jumps across pore bodies. If bubbles are larger than pores, diffusion does not increase average bubble size. Diffusion increases the capillary resistance to flow; the increase is greatest when the characteristic rate of diffusion is close to the convection rate. Diffusion increases capillary resistance to flow because lamellae spend more time in positions of greater curvature than in the absence of diffusion. For characteristic diffusion rates much greater or much less than the imposed convection rate the effect of diffusion on capillary resistance to foam flow is modest.

These results suggest that by itself, an increase in diffusion rate through lamellae does not make foam flow with less resistance. With diffusion lamellae spend more time in pore throats where capillary resistance to flow is greatest.

Contents

1 Introduction

Foams are used in enhanced oil recovery (EOR) to improve gas sweep. Foam blocks gas flow and thereby reduces gas mobility. By reducing the mobility of gas foam increases gas sweep and oil recovery. The pores filled with the foam in the subsurface are believed to be small enough that bubbles are larger than pores (1,2); when this occurs the curved liquid films (lamellae) separating bubbles extend across the pores nearly perpendicular to the pore walls (1,3). Although most bubbles are trapped, some move through these pore spaces under the driving force of convection and/or diffusion, in what is called a “bubble train”. A simple model for foam movement through porous media was already developed by Rossen (4-7), who accounts for the curvature and pressures of bubbles as they move through the pores but doesn’t take into account the effect of diffusion.

As shown by Rossen (4), a minimum pressure gradient is required to overcome the capillary resistance to foam flow and keep these trains moving; this pressure gradient is dependent on pore shape, foam texture (i.e., bubble size), and surface tension. It is thought that about half the mobility reduction in foam arises from the capillary resistance to foam flow (8). The shape of the pores mainly determines the shape and curvature of the lamellae, since lamellae must be nearly perpendicular to the pore walls (3). In 3D these shapes can get very complex when they make jumps in the middle of the pores and take on asymmetric shapes (6). A 2D model simplifies this complexity while retaining the basic trends, as shown by Cox et al. (9) who solved for the lamella shapes moving through a sinusoidal or conical pore in 2D and 3D. Values for film permeability to gas diffusion are given by Farajzadeh et al. (10), who made a study of different gases and surfactant types and their effect on foam film permeability. These values are used here to estimate realistic choices for parameters describing the driving forces in our model.

In a beaker or blender filled with foam, even with no rupture of lamellae, bubbles still grow and shrink due to diffusion. Eventually there is only one big bubble filling the whole of the glass. By analogy, small bubbles, much smaller than pores, shrink and eventually disappear within a pore, leaving only bubbles as large as pores at the end. This has been illustrated for static bubbles in pores (11), but not for bubbles in motion through a pore network. Nor has the effect of diffusion on moving bubbles are already larger than a pore been determined. Here we solve for the effect of diffusion on bubble size and capillary resistance to flow for bubbles somewhat smaller, and larger, than pores, with or without convection, in the context of a simplified 2D model.

2 Progression of a lamella through a pore

Our model of the porous medium is a periodically constricted tube comprising identical bi-conical pores. Because of the complex shapes lamellae take in 3D (9), we follow Rossen (6,7) and assume for simplicity a 2D geometry. For the sake of calculating bubble volumes (instead of areas in 2D) we assume the pore extends a distance h in the third dimension. Like Rossen (6) we assume quasi-static movement, so that lamellae are always perpendicular to the pore wall (except where the pore wall makes a sharp angle); this geometric constraint is approximately correct for moving lamellae (6).

To avoid some complications described below, we place some constraints on pore geometry described here. The parameters defining pore shape are illustrated in Figure 1. The passage of a lamella through this pore is illustrated schematically in Figure 2 (see also (6)).

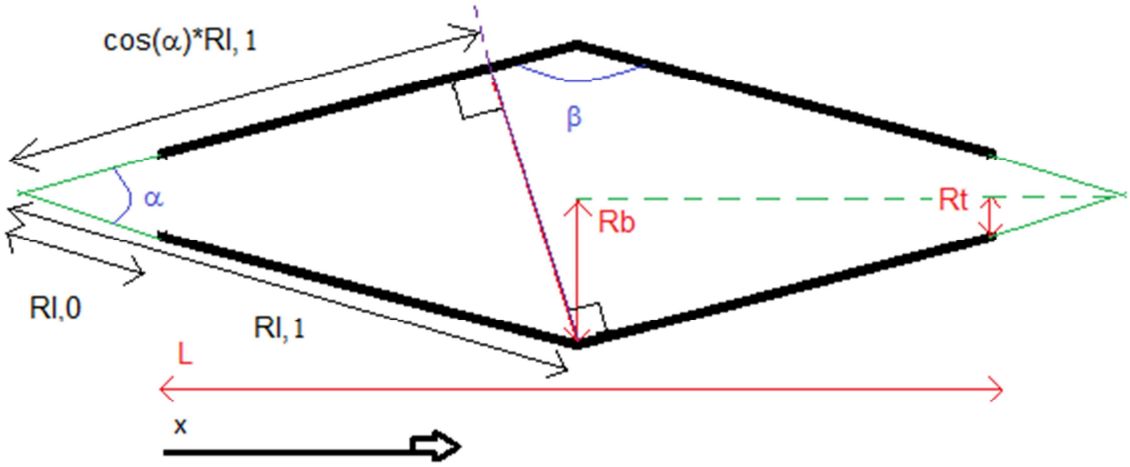

Figure1. Parameters defining pore geometry.

The first constraint we place on geometrical parameters is

$$cos(\alpha)\, R_{l,1} > R_{l,0} \qquad [2\text{-}1]$$

This ensures that when the lamella jumps in the pore body (from Interval 2 to 3 in Figure 2), it attaches to the flat, parallel pore walls on both sides of the pore, rather than the upstream pore throat. Thus for all of interval 3 the lamella is flat. Our second constraint is

$$R_b - R_t \leq \frac{L}{2} \qquad [2\text{-}2]$$

This statement implies that the angle at the pore body is greater than 90º, and thus the lamella touches the opposite pore wall at its ends and does not touch the opposite pore wall within the arc of the lamella:

$$\frac{\pi}{2} \leq \beta \leq \pi \qquad [2\text{-}3]$$

$$\alpha \leq \frac{\pi}{2} \qquad [2\text{-}4]$$

We define dimensionless body and throat radii as follows:

$$\rho_b = \frac{2R_b}{L} \qquad [2\text{-}5]$$

$$\rho_t = \frac{2R_t}{L} \qquad [2\text{-}6]$$

We next consider the movement of the lamella forward through the pore in five intervals, illustrated in Figure 2.

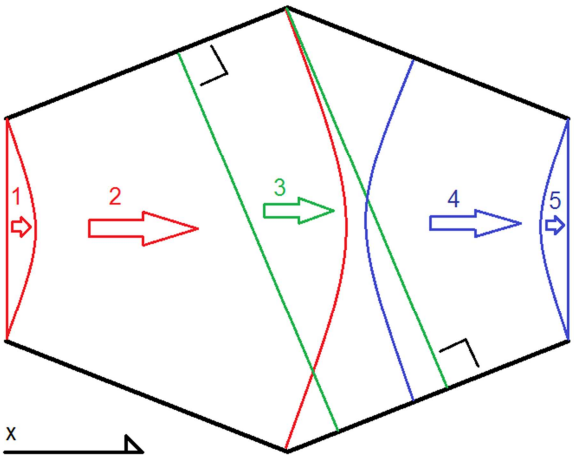

Figure 2. Schematic of lamellae movement through pore. Numbers refer to intervals explained in text.

2.1 Interval 1: lamella bulges forward in throat

This phase can be viewed in two ways, namely as the increase of the angle ω the lamella makes with the vertical at the pore corner or the decrease from an infinitely large radius (for a flat lamella) to R_{l0}, the minimum radius of the lamella during its passage through the pore. We parameterize this interval in terms of the angle ω, as illustrated in Figure 3.

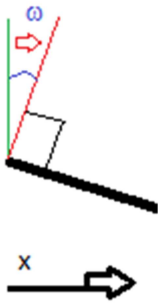

Figure 3. Increasing angle of lamella in pore throat.

As the lamella bulges forward as shown in Figure 3, the volume is calculated from the equation for a segment of a circle (12):

$$V_1 = \frac{1}{2} R_{l,0}^2 [2(\omega) - sin(2\omega)] h \qquad [2.1\text{-}1]$$

V_1 is the volume behind the lamella in terms of ω. During this interval ω increases from 0 to (α/2), and the radius of the lamella is $R_l=R_t/\sin(\omega)$. Also h is used as a parameter for the 3th dimension.
At the start of interval 1, R_l is infinite, and at the end, $R_l=R_{l,0}=R_t/\sin(\alpha/2)$, its minimum value during passage through the pore. The volume behind the lamella at the end of Interval 1 is given by Eq. 2.1-2 with ω = (α/2):

$$V_{1,max} = \frac{1}{2} R_{l,0}^2 [\alpha - sin(\alpha)] h \qquad [2.1\text{-}2]$$

2.2 Interval 2: lamella moves among diverging pore wall

Interval 2 is the progression of the lamella to the middle of the pore. During this movement the lamella makes an angle of $\pi/2$ with the pore wall and an angle ($\alpha/2$) with the vertical.

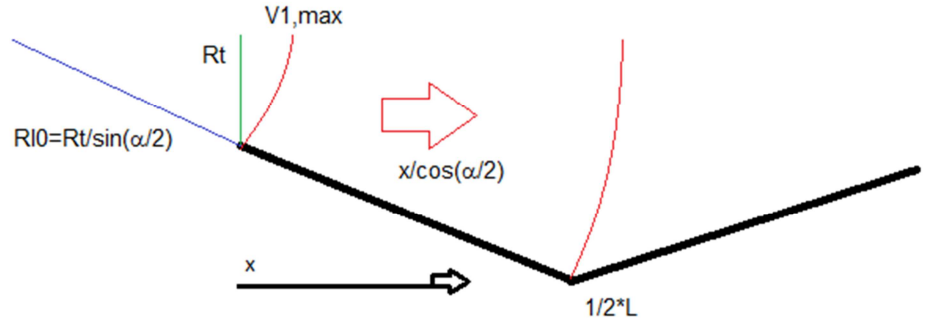

Figure 4. Lamella moving forward along diverging pore wall.

As shown in Figure 4 the lamella moves from position of attachment to the pore wall x=0 to x=(L/2). The radius of the lamella is;

$$R_l = \left(\frac{R_t}{sin(\frac{\alpha}{2})}\right) + \left(\frac{x}{cos(\frac{\alpha}{2})}\right) \quad [2.2\text{-}1]$$

And the volume behind the lamella, V_2, is given by;

$$V_2 = V_{1,max} + \left(\frac{\alpha}{2}\right)\left(R_l^2 - R_{l,0}^2\right) h \quad [2.2\text{-}2]$$

In Eq. 2.2-2, V_2 is the volume behind the lamella and is equal to sum of the volume at the end of interval 1, $V_{1,max}$, and the volume in the annular region behind the lamella, as illustrated in Figure 4. In this interval ω is at its maximum value ($\alpha/2$), acquired in Interval 1 and R_l is the radius of the lamella, which increases with increasing x as shown in Figure 4.

The minimum and maximum values of R_l in this interval, namely $R_{l,0}$ Eq. 2.2-3 and $R_{l,1}$ Eq.2.2-4, respectively, are the values of R_l as the lamella leaves the pore throat and as it arrives at the corner at the pore body (x=L/2). They are given by;

$$R_{l,0} = \frac{R_t}{sin(\frac{\alpha}{2})} \quad [2.2\text{-}3]$$

$$R_{l,1} = \frac{R_t}{sin(\frac{\alpha}{2})} + \left[\frac{\frac{L}{2}}{cos(\frac{\alpha}{2})}\right] \quad [2.2\text{-}4]$$

Therefore the maximum volume acquired for V_2 is given as follow;

$$V_{2,max} = V_{1,max} + \left(\frac{\alpha}{2}\right)\left(R_{l,1}^2 - R_{l,0}^2\right) h \quad [2.2\text{-}5]$$

2.3 Interval 3: jump and asymmetric shapes

As the lamella radius gains its maximum value in Interval 2, $R_{l,1}$, it next jumps to a new position with a same bubble volume (6). In 3D this shape is complex (6,9), but in our simple 2D pore the lamella is flat. When this is true then the cross-sectional area of the bubble is composed of a large triangle minus a small one, plus a rectangle, as shown in Figure 5, and volume is given by

$$V_3 = \left[\left(\frac{1}{2} R_{l,1}^2 \, sin(\alpha) \, cos(\alpha) - R_t \, R_{l,0} \, cos(\frac{\alpha}{2})\right) + sin(\alpha) \, R_{l,1} \frac{(x - \frac{L}{2})}{cos(\frac{\alpha}{2})}\right] h \quad [2.3\text{-}1]$$

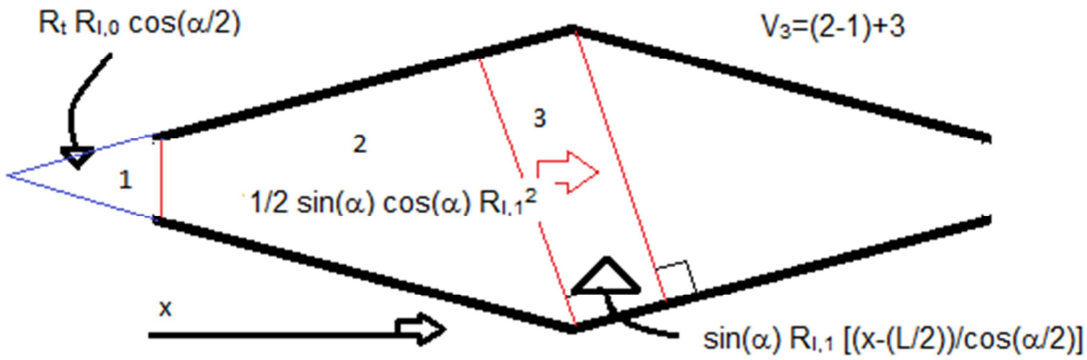

Figure 5. Geometric formulas used in computation of bubble volume in Interval 3.

The lamella jumps to a position part-way along the converging pore wall, as illustrated in Figure 2. The new volume, given by Eq. 2.3-1, equals the final volume of Interval 2, given by Eq. 2.2-5. Knowing that $V_{2,max}$ equals the initial value of V_3, gives the initial value of x Eq. 2.3-2 (the position of lamella attachment to the converging pore wall) in this interval, which we call x_1:

$$x_1 = [\frac{V_{2,max}}{h} - (\frac{1}{2} R_{l,1}^2 \, sin(\alpha) \, cos(\alpha) - R_t \, R_{l,0} \, cos(\frac{\alpha}{2}))] \frac{cos(\frac{\alpha}{2})}{sin(\alpha) \, R_{l,1}} + \frac{L}{2} \quad [2.3\text{-}2]$$

The maximum value of x in this interval is x_2, which is determined by the condition that the other side of the lamella contacts the corner at the pore body (Figure 6):

$$x_2 = \frac{1}{2} L + [R_{l,1} - cos(\alpha) \, R_{l,1}] \, cos(\frac{\alpha}{2}) \quad [2.3\text{-}3]$$

In Eq. 2.3-3 the term in brackets represents the distance between the red lines around region 3, in Figure 5. By multiplying this by the cosine term it is translated into position x. So x_1 lies between the pore body (L/2) and x_2, depending on the geometrical parameters of the pore, as illustrated in Figure 6.

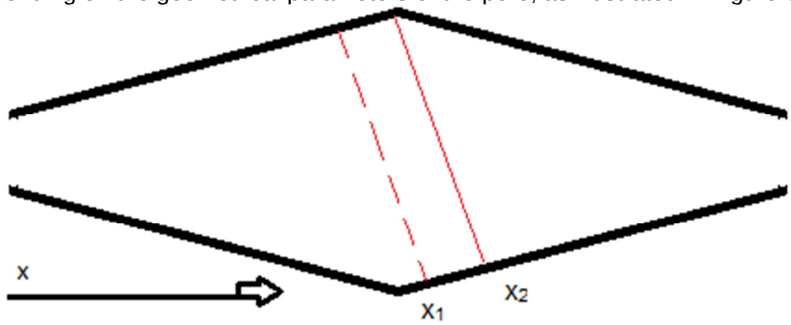

Figure 6. Illustration of x_1 and x_2 in Interval 3.

So when the lamella reaches x_2, V_3 reaches its maximum value. The expression for $V_{3,max}$ is given by Eq. 2.3-4;

$$V_{3,max} = [(\frac{1}{2} sin(\alpha) \, cos(\alpha) \, R_{l,1}^2 - R_t \, R_{l,0} \, cos(\frac{\alpha}{2})) + sin(\alpha) \, R_{l,1} \frac{(x_2 - \frac{L}{2})}{cos(\frac{\alpha}{2})}] \, h \quad [2.3\text{-}4]$$

2.4 Interval 4: second jump and lamella movement up converging pore wall

This interval starts when the trailing edge of the lamella jumps from the pore body to the converging pore wall. In essence this interval is the same Interval 2, except that curvature is reversed and the volume of interest is the volume on the concave side of the lamella. Figure 7 shows that the lamella is now bulging backward.

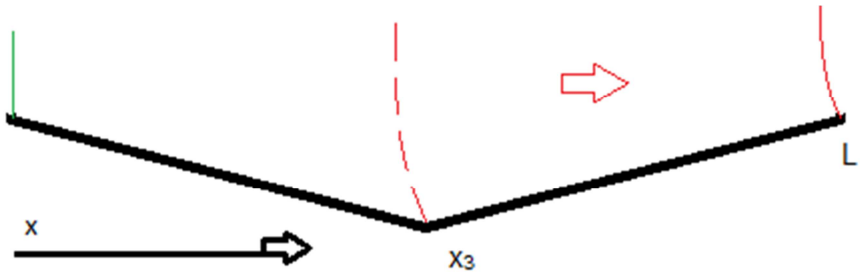

Figure 7. Lamella advancing up converging pore wall.

The bubble volume in interval 4 is given by;

$$V_4 = V_{tot} - V_{1,max} - h\left(\frac{\alpha}{2}\right)\left[\left(R_{l,0} + \frac{(L-x)}{cos(\frac{\alpha}{2})}\right)^2 - R_{l,0}^2\right] \quad [2.4\text{-}1]$$

With;

$$V_{tot} = (R_b + R_t)\, L\, h \quad [2.4\text{-}2]$$

This is the inverse result of Eq. 2.2-2. V_{tot} represents the total volume of the pore Eq. 2.4-2 and $V_{1,max}$, Eq. 2.1-2, the maximum volume in Interval 1. The initial value of x, x_3, is determined by equating the volume given by Eq. 2.4-1 to the maximum volume in Interval 3, Eq. 2.3-4; the result is as follows:

$$x_3 = -\left[\sqrt{\left(\frac{V_{3,max} - V_{tot} + V_{1,max}}{-h}\frac{2}{\alpha} + R_{l,0}^2\right)} - R_{l,0}\right] cos\left(\frac{\alpha}{2}\right) + L \quad [2.4\text{-}3]$$

The maximum bubble volume in Interval 3, $V_{3,max}$, is given by Eq. 2.3-4. $V_{1,max}$ is given by Eq. 2.1-2. From x_3, x increases to L. It is true that $x_2 > x_3$, but this means only that the leading edge of the asymmetric lamella jumps back a bit at the jump, while the bubble retains the same volume with this new shape.

2.5 Interval 5: lamella in downstream pore throat

Interval 5 is the inverse of Interval 1, with the lamella making a decreasing angle with the vertical. During this transition lamella radius increases from $R_{l,0}$ to infinity, i.e. a flat shape in the pore throat. The volume in this interval can be represented by

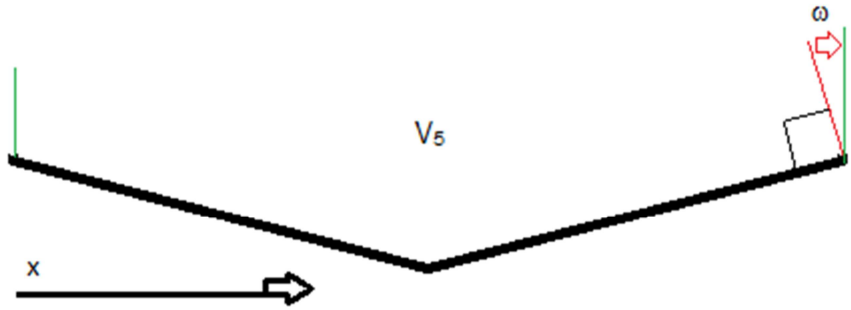

Figure 8. Lamella in downstream pore throat.

$$V_5 = V_{tot} - \frac{1}{2}R_{l,0}^2[(2\omega) - sin(2\omega)]\, h \quad [2.5\text{-}1]$$

Angle ω decreases from its maximum value to zero, at which point the lamella is flat. This is the inverse of Eq. 2.1-1, as shown in Figure 8.

3 Pressure, convection and diffusion

In the previous section the sequence of lamella shapes was described, in particular relating lamella radius R_l to bubble volume V. These properties are crucial to estimating bubble pressure, capillary resistance to flow, and diffusion rate.

3.1 Pressure

Since this is a 2D model, the capillary entry pressure (P_c^e) is given by surface tension divided by the pore throat radius (γ/R_t) and the pressure difference between bubbles ΔP by ($2\gamma/R_l$). We define dimensionless pressure difference (ΔP_D) as ($\Delta P/P_c^e$). Therefore, $\Delta P_D = (2R_t/R_l)$. The same formula would apply in 3D, where R_l would reflect mean curvature of the lamella. By convention R_l is defined as negative when the lamella bulges backwards in Intervals 4 and 5. The volume is made dimensionless by dividing by the total volume V_{tot}.:

$$V_D = \frac{V}{V_{tot}} \qquad [3.1\text{-}1]$$

With these definitions and the equations in the previous section one can relate dimensionless pressure difference between bubbles to bubble volume and lamella position. As noted, ΔP_D is zero in Interval 3 and negative in intervals 4 and 5. It is also zero at the start and end of the lamella's passage through the pore. Figure 9 relates dimensionless pressure difference to dimensionless volume for the geometrical pore parameters given in Section 4.2. Using Figure 9, the positions and pressure differences across all lamellae in a bubble train can be reconstructed, by representing the position of each lamella in its pore in terms of cumulative volume from the start of the train to the given lamella. Details are given below.

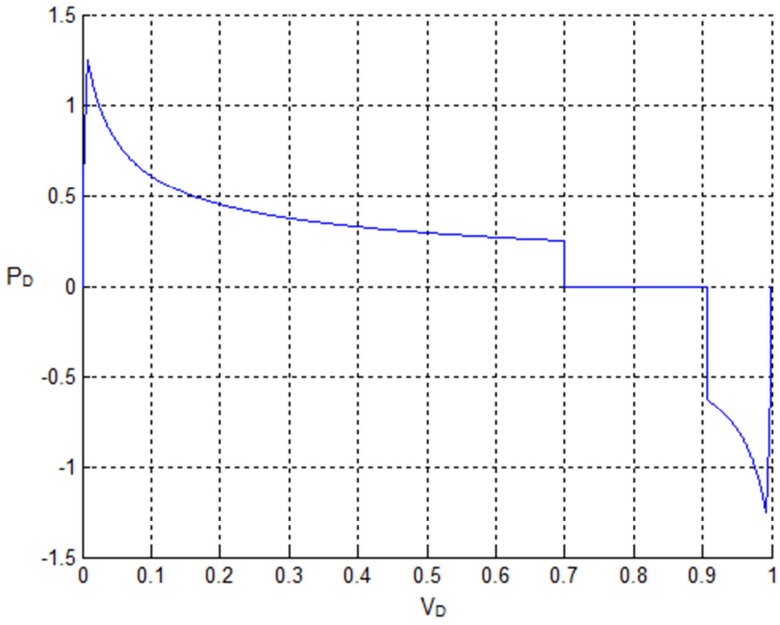

Figure 9. Dimensionless pressure difference across a lamella P_D vs dimensionless volume V_D. The average value is 0.2165; stdev, 0.4153.

Similar graphs are shown by Cox et al. (9), who also made them for various 3D pore and lamella shapes. In the 3D results from Cox et al. (9), the constant, zero value of P_D in Interval 3 is replaced by a trend of nonzero and increasingly negative P_D. In 3D the lamella is not flat; it takes a saddle shape, with increasingly negative curvature as more of the circumference of the lamella touches the converging pore wall. Two of the plots of Cox et al. are given in Appendix A.

3.2 Movement

Diffusion is defined as a mass flux across a lamella, but for simpler comparison to convection we define it as a volume ΔV_{diff} transported in a time increment Δt. We assume that the gas inside the bubbles is an ideal gas, overall gas pressure (used to relate volume to mass in the ideal gas law) is nearly constant in spite of pressure differences between bubbles, and that diffusion across lamellae is characterized by a constant film permeability K; and we ignore any effect of Plateau borders on diffusive transport, just as we have neglected any effect on lamella shape above. We start by considering diffusive transport in Interval 2:

$$\Delta V_{diff} = \frac{K A \Delta C_g \Delta t}{V_m} = \frac{K \alpha h R_l \frac{\Delta P}{RT} \Delta t}{\frac{P}{RT}} = \frac{K \alpha h \frac{4\gamma}{\Delta P} \frac{\Delta P}{RT} \Delta t}{\frac{P}{RT}} = K \alpha h \frac{4\gamma}{P} \Delta t \qquad [3.2\text{-}1]$$

ΔV_{diff}	change in volume due to diffusion [m^3]; positive if downstream bubble grows in volume
K	film permeability to gas diffusion [m/s]
A	lamella area [m^2]
ΔC_g	concentration difference of gas on both sides of the lamella [mol/m^3], equal to $\Delta P/RT$
Δt	time increment [s]
V_m	molar volume [m^3/mol]
α	angle defined in Figure 1 [rad]
h	depth of 2D pore in 3D [m]
R_l	radius lamella (assuming lamella is in Interval 2; other cases shown discussed below) [m]
ΔP	pressure difference across the lamella [N/m^2], equal to $4\gamma/R_l$
R	ideal-gas constant [Nm/mol/K]
T	temperature [K]
P	*in situ* pressure [N/m^2]
γ	surface tension [N/m]

Note that this Eq. 3.2-1 is derived for interval 2, but can be applied also to interval 4 where it would have a negative sign to account for the reversed curvature of the lamella. In Intervals 2 or 4, the change in lamella area, proportional to R_l, is balanced by changes in curvature ($1/R_l$), and diffusion rate is the same for all locations within the interval. We use this constant reference rate in Eq. 3.2-1 to compute the rate of transport in each interval below. In 3D, lamella area is proportional to R_l^2, and diffusive transport rate is not constant in Intervals 2 or 4; the maximum diffusion rate happens just before the lamella jumps at the pore body.

In interval 3, the lamella is flat, and the rate of diffusive transport is zero.

In Intervals 1 or 5, the area doesn't change nearly as much as curvature changes with the bulging or flattening of the lamella in the throat. Therefore, to simplify the calculation of diffusive transport in Intervals 1 and 5, we assume that lamella area is constant at its value at the boundary between intervals 1 and 2 or 4 and 5, respectively. The rate of diffusive transport is then the same constant rate as in Intervals 2 and 4, but scaled by the reduced curvature ($R_{l,0}/R_l$), with a negative sign in Interval 5 as in Interval 4. This results in the following formulas for diffusive transport rate in the different intervals:

Interval 1: $$\Delta V_{Diff,1} = \frac{R_{l,0}}{R_l} \Delta V_{Diff} \qquad [3.2\text{-}2]$$

Interval 2: $$\Delta V_{Diff,2} = \Delta V_{Diff} \qquad [3.2\text{-}3]$$

Interval 3: $$\Delta V_{Diff,3} = 0 \qquad [3.2\text{-}4]$$

Interval 4: $$\Delta V_{Diff,4} = -\Delta V_{Diff} \qquad [3.2\text{-}5]$$

Interval 5: $$\Delta V_{Diff,5} = -\frac{R_{l,0}}{R_l} \Delta V_{Diff} \qquad [3.2\text{-}6]$$

We represent convection as a constant, externally constrained, positive volumetric flow rate of gas. In effect, like Rossen (4), we assume pistons upstream and downstream of the bubble train, advancing at a constant rate. Assuming that the volume increment to lamella positions ΔV_{conv} from the advance of these pistons over a time increment Δt is some fraction C of the volume of one pore V_{tot}, we have;

$$\Delta V_{conv} = C V_{tot} = \frac{C}{\Delta t} V_{tot} \Delta t \qquad [3.2\text{-}7]$$

Superficial velocity v is the length of a pore divided by the time it takes a pore volume of gas to be injected; hence

$$\Delta V_{conv} = (\frac{v V_{tot}}{L})\Delta t \qquad [3.2\text{-}8]$$

Combining these two relations we arrive at a definition of dimensionless time based on convection rate:

$$\frac{C}{\Delta t} = \frac{v}{L} \Rightarrow C = \frac{\Delta t\, v}{L} = \Delta t_D \qquad [3.2\text{-}9]$$

Where;

v	superficial velocity [m/s]
C	constant defined by Eq. 3.2-7 [-]
L	length of the pore [m]
Δt	time step [s]
Δt_D	dimensionless time per time step [-]

In a situation where there is no convection, dimensionless time must be based on ΔV_{diff}. For such cases we define dimensionless time based on the amount of diffusive gas transport in a time increment Δt (assuming a lamella in Interval 2 or 4) (cf. Eq. 3.2-1):

$$\Delta t_{D,diff} = \frac{\Delta V_{diff}}{V_{tot}} = \frac{K\,\alpha h 4\gamma\,\Delta t}{P V_{tot}} \qquad [3.2\text{-}10]$$

For cases with both convection and diffusion, we define a ratio of the two rates, again based on the diffusion rate in Interval 2:

$$F_{dc} \equiv \frac{\Delta t_{D,diff}}{\Delta t_{D,conv}} = \frac{K\,\alpha h 4\gamma\,\Delta t}{P V_{tot}} \frac{L}{v\,\Delta t} = \frac{K\,\alpha h 4\gamma\, L}{P V_{tot}\, v} = \frac{4\,K\,\alpha\,\gamma}{P(R_b + R_t)v} \qquad [3.2\text{-}11]$$

The ratio of diffusive to convective flux increases with film permeability K, as expected, and surface tension (driving the pressure differences between bubbles); for pores of a given geometry, the ratio decreases with increasing size of the pores, with increasing pressure (meaning a given molar flux of gas makes less difference to bubble volume) and with increasing superficial velocity v. It is important to note that v here is superficial velocity of the *flowing* gas fraction, not the superficial velocity of the gas phase averaged over all the trapped gas. Flowing gas saturation can be as little as 1% of total gas saturation (13), and v here reflects the velocity of gas that actually flows.

For cases with both convection and diffusion we use t_D based on convection in Eq. 3.2-9, and relate diffusion rate to convection rate using the ratio F_{dc} from Eq. 3.2-11. For cases with no convection, we use dimensionless time based on diffusion (Eq. 3.2-10).

3.3 Merging of lamellae

It is well known that in bulk foams small bubbles disappear by gas diffusion into larger surrounding bubbles. Cohen et al. (11) show that, in the absence of convection small bubbles lodged in pore throats disappear by gas diffusion out of these bubbles. Here we find another mechanism of bubble disappearance in porous media: lamellae between sufficiently small bubbles come into contact at the jumps at the pore body, between intervals 2 and 3 or between intervals 3 and 4 (see Fig. 2). After this, the small bubble is lodged against the pore wall (see Figure 10), where it is bypassed by convection and it disappears over time by diffusion. We do not attempt to represent the diffusion process for the bypassed bubble in detail. Instead, when lamellae intersect each other immediately after a jump, the rearward lamella of these is (in this model) deleted from the list of lamellae.

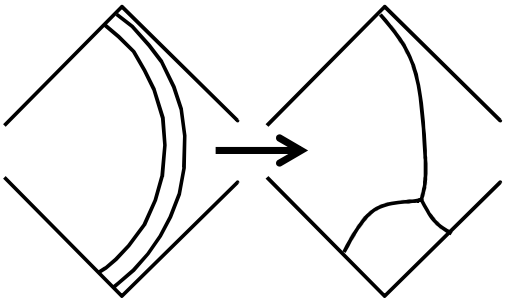

Figure 10. Schematic of the result of lamellae that would overlap when the forward lamella jumps from the pore body to an asymmetric shape. One edge of the lamella moves backwards (Figure 2), where it meets the lamella behind it; the bubble between these lamellae is isolated to the pore body, where it subsequently disappears by diffusion.

In addition, if bubbles are sufficiently close to each other on the pore wall that their Plateau borders overlap, one of the bubbles would be shunted toward the opposite pore wall and bypassed by subsequent convection. The sort of rearrangement shown in Figure 10 could thus also be triggered by overlapping Plateau borders away from a pore body.

We do not attempt to represent the diffusion process for the bypassed bubble in detail. Instead, we eliminate the rearward lamella immediately when any of the following situations occurs:

- When a lamella from Interval 3 intersects a bubble bulging either forward or backward from Intervals 2 or 4. The intersection is indicated by the lamella of the forward bubble contacting one of the pore walls at a point behind that of the forward lamella.
- When lamellae next to each other have a dimensionless volume difference less than 0.05 (to schematically represent isolation of bubbles as a result of overlapping Plateau borders).
- For other pore shapes, lamellae from Intervals 2 and 4 could intersect in the middle of the pore, but this can't happen with the geometric constraints on pore shape we have imposed.

The most common situations are the first 2. The implementation of these checks in Matlab®, The MathWorks, Inc., Natick, Massachusetts, United States. can be found in Appendix in the section of the Matlab® code denoted **%% incr/decr Vrt.**

4 Train of Bubbles

In previous sections it was explained how individual lamellae can be represented mathematically as they move through a pore, and how the pressure difference between bubbles and convection and diffusion rates are represented in this model. Now we consider multiple pores and multiple bubbles in a bubble train.

4.1 Method of calculation

To start it is needed to set the initial positions of the lamellae. Therefore a table relating the volumetric position of a lamella in a pore V_D to the corresponding value for ΔP_D is needed; the graphical representation of this table is Figure 9. To assign initial positions for the lamellae individual dimensionless bubble volumes are randomly picked from a uniform distribution. The distribution extends from 0 to 1 for when the bubbles are initially smaller than the pores and from 1 to 2 for bubbles larger than a single pore. The latter case represents bubbles larger than 2 pores as well; for any bubble volumes greater than one pore, consecutive lamellae to not occupy the same pore. In our calculations, we assume 300 bubbles in the train.

The initial volumetric position of lamella n is given by the sum of the n volumes of the bubbles 1 to n. The position of lamella n within its given pore is the decimal portion of this total. From the volumetric position the dimensionless pressure difference across each lamella is determined by interpolation from the tabular representation of Fig. 9. The positions of lamellae attachment to the pore walls can also be determined from the formulas in Section 2, and a check made for intersecting lamellae or lamellae close enough to each other that they would merge.

The flow chart for the calculation of the advance of the bubble train can be found in Appendix B, Figure B1. All examples here use the geometric parameters in the next section. Lamellae move forward or backward in every iteration step; the movement depends on the values assigned to the convection and diffusion rates. The increment in dimensionless time in each step can't be too large or else the lamella might skip whole intervals in a single iteration step, resulting in false conclusions and incorrect behavior. In each result below the dimensionless time step used in the calculation is given.

One check to the method of calculation is modeling a single bubble cross a pore, with no diffusion, and monitor its progress. A plot of ΔP_D vs V_D results in Figure 11. The sum of the values of P_D at each time step, divided by the number of time increments, should match the integral (i.e., average value of P_D) from Figure 9. As expected, the values match closely. The slight difference in average can be solved by decreasing the time step.

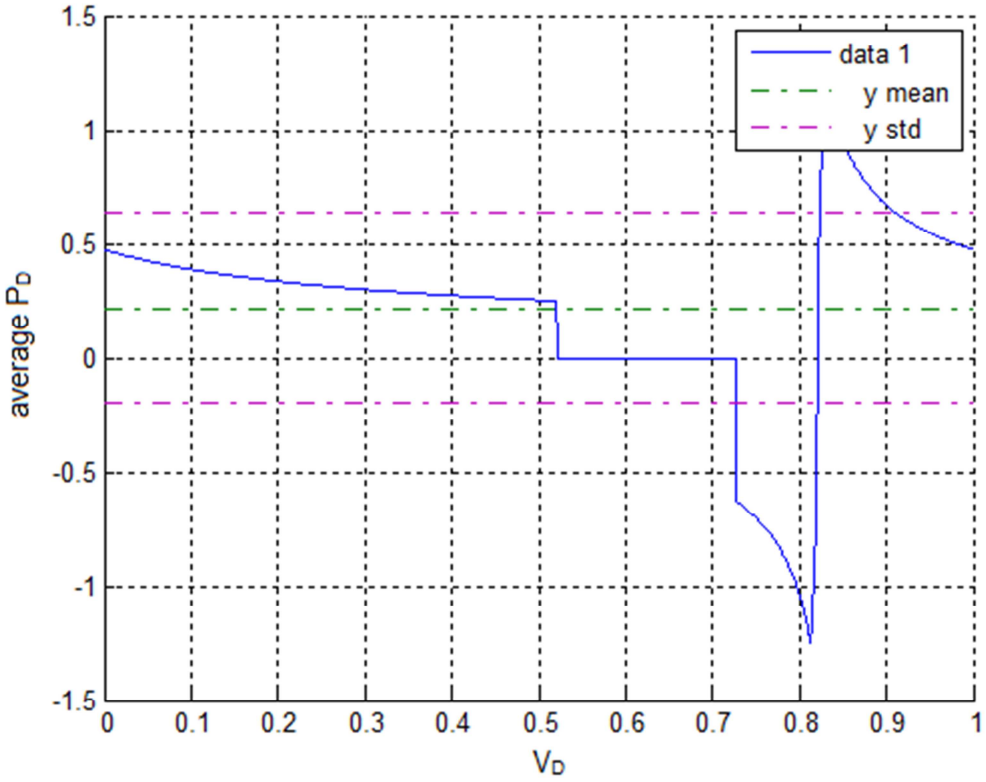

Figure 11. One randomly selected lamella crosses a single pore. Its initial position is in Interval 2. The average value of P_D is 0.2166 and the standard deviation 0.4154.

Bubbles initially smaller than pores, with dimensionless bubble volumes between 0 and 1, can cross each other or can be too close to one other according to the criteria in Section 3.3, even as initially assigned.

Then the rearward lamella is made zero, and thereby deleted from the distribution. From the second statement there, forward lamella is just 0.05 V_D larger, one can expect that, when lamellae smaller than pores are picked that ~5% will initially be to close. For 300 lamellae that would mean 15 lamellae would be merging right away from this specific statement alone. In general this is a good approximation but also other lamellae from interval 2 or 4 will merge from initially overlapping with a lamella from interval 3, as it happens this varies much for each distribution from just 5 to 20 lamellae. So initially, around 20 to 35 bubbles are expected to merge when working with bubbles smaller than pores.

An example of an initial bubble size distribution (BSD) when the bubbles are larger than the pores can be seen in Figures 12 and 13. In Figures 12 and 13 the initial bubble sizes are randomly distributed between 1 and 2; therefore the 300 bubbles occupy about 450 pores, since the average bubble volume is 1.5 pores. According to the Central Limit Theorem of statistics, the average P_D for 300 bubbles should be the expected value for one bubble plus or minus about twice the standard deviation for one bubble divided by $\sqrt{300}$. The population average for the 300 bubbles falls within this range. For bubbles with initial size randomly distributed between 0 and 1, the 300 bubbles would fill 150 pores, since average initial volume of a bubble is then 0.5.

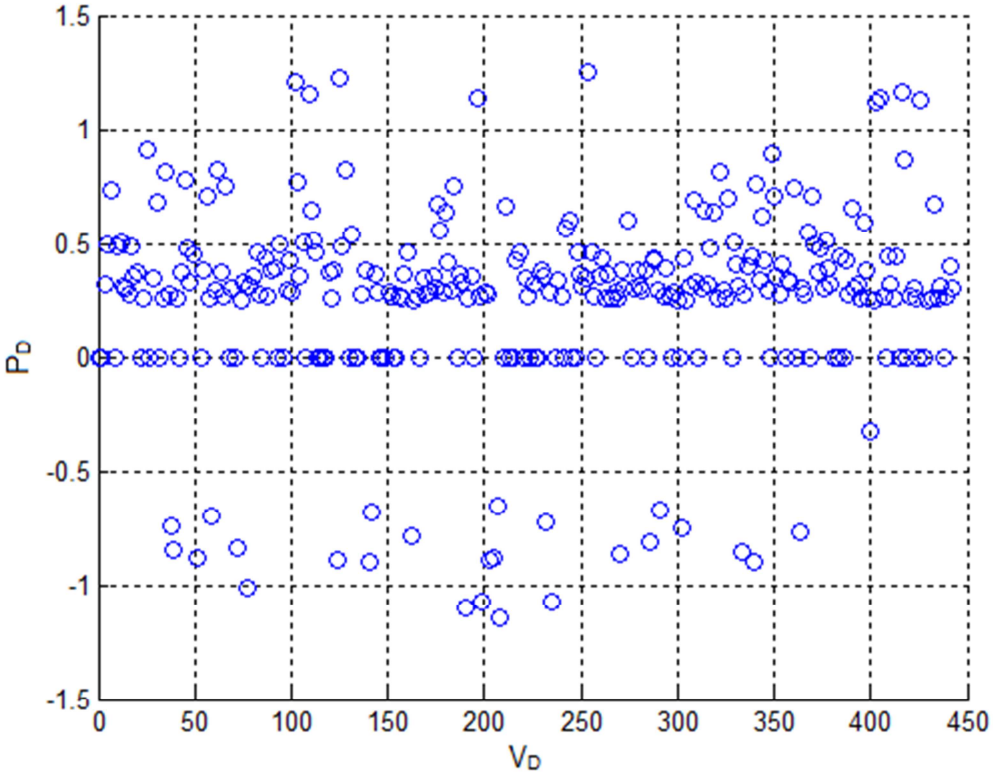

Figure 12. Initial distribution of values of P_D for 300 bubbles with bubble volumes randomly chosen from a uniform distribution between 1 and 2.

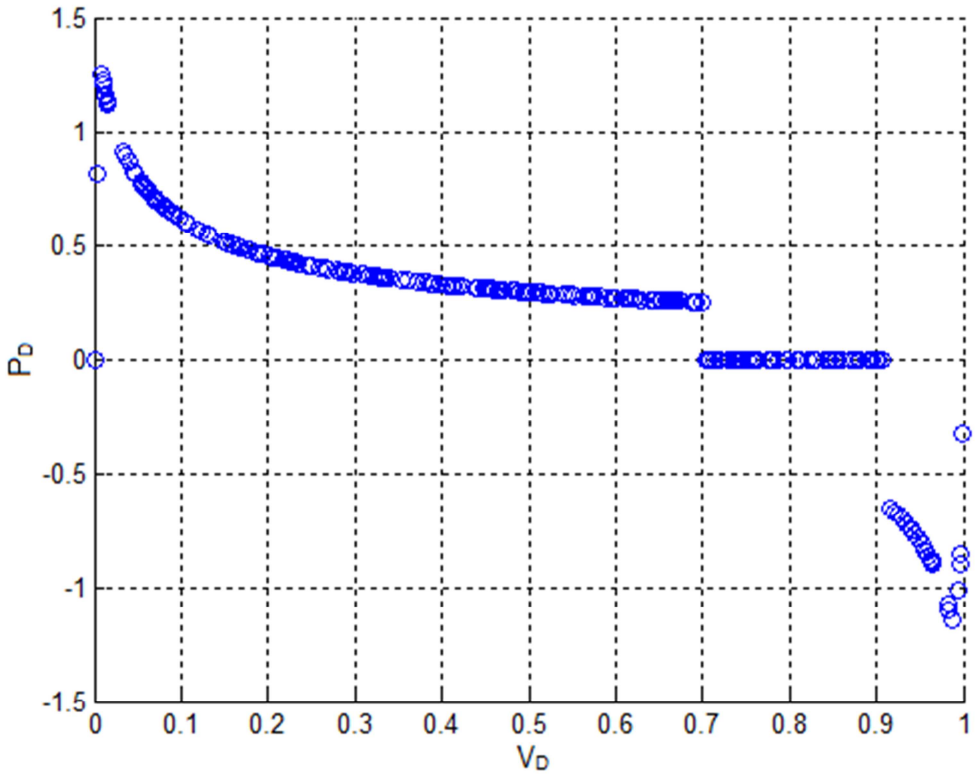

Figure 13. Initial bubble distribution from Figure 12 projected in terms of P_D vs volumetric position of lamella in the given pore; mean=0.2388; standard deviation=0.4202.

One aspect of this distribution is that the presence or absence of a small number of lamellae in or near the pore throats can have a noticeable impact on the pressure difference across the whole train. This is reflected in the large value of standard deviation for P_D for one lamella.

4.2 Parameter values selected

For the dimensionless geometry of the pore used it is only needed to select the length and body/throat radius; the model then determines the angles in Figure 1. For all the examples in this thesis the following values are used:

R_t	10 μm
R_b	50 μm
L	100 μm
β	~102.7^0
ρ_t	0.2
ρ_b	1
α	0.9

The model calculates the remaining pore parameters required to set up a table consisting of P_D and V_D values. All the calculations are dimensionless, but the ratio of diffusion to convection rates F_{dc} depends on dimensional quantities. Values for film permeability and surface tension at low pressure are available from Farajzadeh et al. (10); for CO_2 and N_2 gases representative values are 7.85 x 10^{-2} and 1.31 x 10^{-3} m/s for film permeability and 0.025 N/m for surface tension. (Surface tension can be 5 to 10 times lower for supercritical CO_2 (4) To put bounds on possible values, consider two extreme cases: a CO_2 foam at 5 bar pressure with superficial velocity of flowing gas of 5 m/d (5.79 x 10^{-5} m/s), and an N_2 foam at 40 bar pressure with flowing-gas superficial velocity of 100 m/d (because of small flowing gas fraction), together with the geometric factors above. Now using Eq. 3.2-11 one obtains F_{dc} = 4.07 and 4.23 x 10^{-4}, respectively for the two cases. Thus even for flowing foam it is conceivable that the characteristic diffusion rate could be faster than the imposed convection rate, at least at relatively low pressure in the laboratory. At 335 K temperature and 100 bar pressure for supercritical CO_2, surface tension is between 0.003 and 0.005 instead of 0.025 N/m (1), and a compressibility factor Z=0.54; even for the same film permeability, F_{dc} is 0.013 instead of 4.07. Thus it is unlikely that in field application of foam F_{dc} is close to 1. Of course if convection stops then all lamella movement is from diffusion.

5 Results

Here we present results for trains of 300 bubbles. The Matlab® code for the calculations can be found in Appendix B.

5.1 No Diffusion

For bubbles larger than pores, without diffusion bubbles simply move forward a constant volumetric amount in each time increment. Therefore one expects that the population-average P_D over the period as bubbles move through a single pore is exactly the same as the integral over the corresponding P_D vs. V_D plot in Figure 9; the train is simply the summation of identical bubbles making identical passages through identical pores (except for the different starting places). One further expects no change in the bubble size distribution. For a population of 300 bubbles one further expects that the standard deviation of population-average P_D would be $1/\sqrt{300}$ times that for a single lamella, and that 95% of the time the population-average P_D lays within twice this a standard deviation of the mean. We find this to be the case (Figure 14).

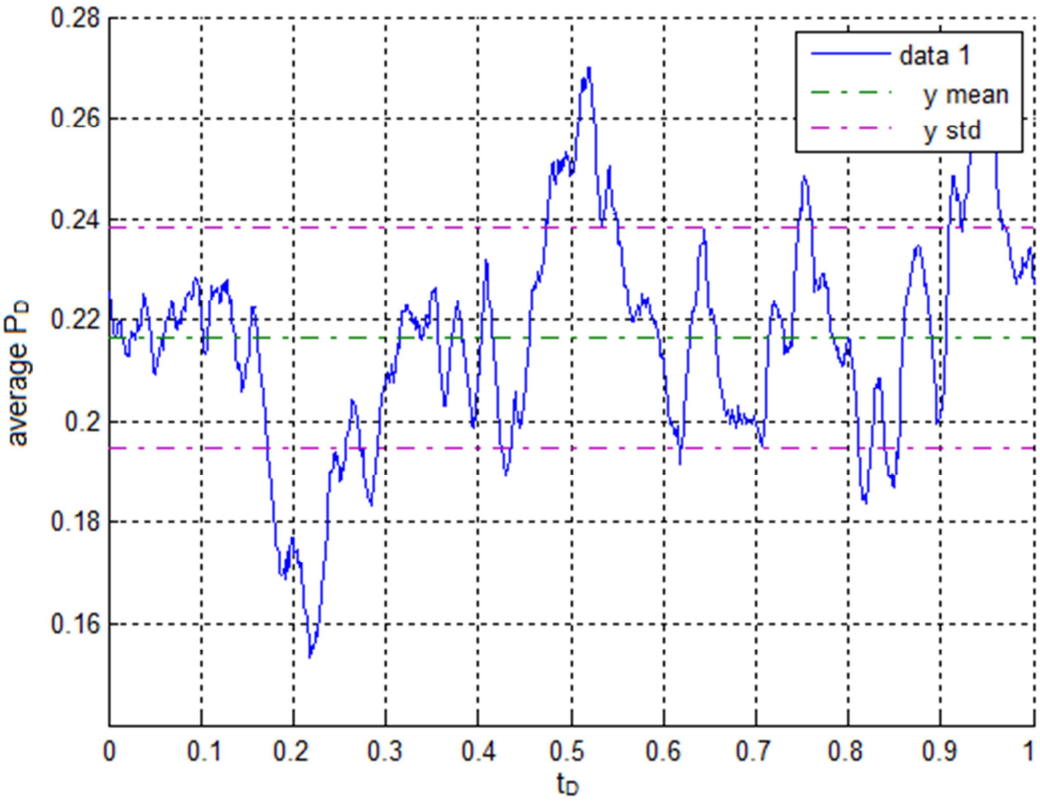

Figure 14. Progress of a train of bubbles larger than pores: mean= 0.2165; stdev.=0.02185; Δt_D=0.001; F_{dc}=0. All lamellae cross 1 pore in the 1000 time steps shown.

It is in principle possible, but unlikely, that average P_D becomes negative for a train of 300 bubbles. According to the Central Limit Theorem, population-average P_D = 0 would lie within two standard deviations of the population mean for a train of about 15, but not 300, bubbles. More important, for trains of 15 bubbles, excursions to twice the average capillary resistance to flow would be fairly common, at which point the given train might be immobilized and other trains mobilized. Once a train is immobilized, lamellae seek out pore throats, as shown in the next section, and capillary resistance to subsequent movement increases.

When the bubbles generated are initially smaller than the pores, some of the lamellae will merge due to their initial positioning, as explained in paragraph 4.1. This effect is also true for Figure 15 but additionally to the initial merging of the lamellae, here 25 lamellae merge initially. But when they start moving another 42 lamellae merge due to the jump from interval 2 to 3 and the jump from 3 to 4. The merging only happens when the lamellae cross their first whole pore, after that the lamellae in this model have and maintain enough space between each other to avoid merging at their current Δt_D and F_{dc}.

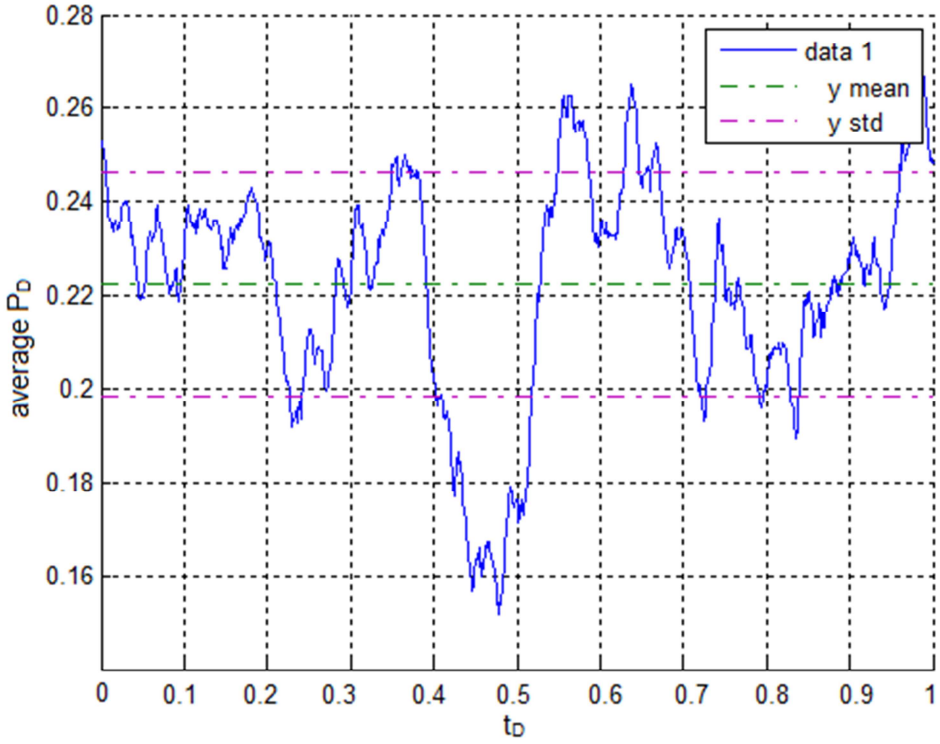

Figure 15. Progress of a train of bubbles initially smaller than pores: mean=0.2224; stdev.=0.02399; Δt_D=0.001; F_{dc}=0. Also 25 bubbles merge at the start (an immediate result of the initial distribution) and 42 additional bubbles merge during movement through the first pore.

Beyond this point, movement through each additional pore is identical, and in the absence of diffusion no remaining bubbles would merge, as shown in Figure 16. Here the average P_D is exactly as for one lamella, because all remaining lamellae make identical passages through one pore (except for the different starting positions).

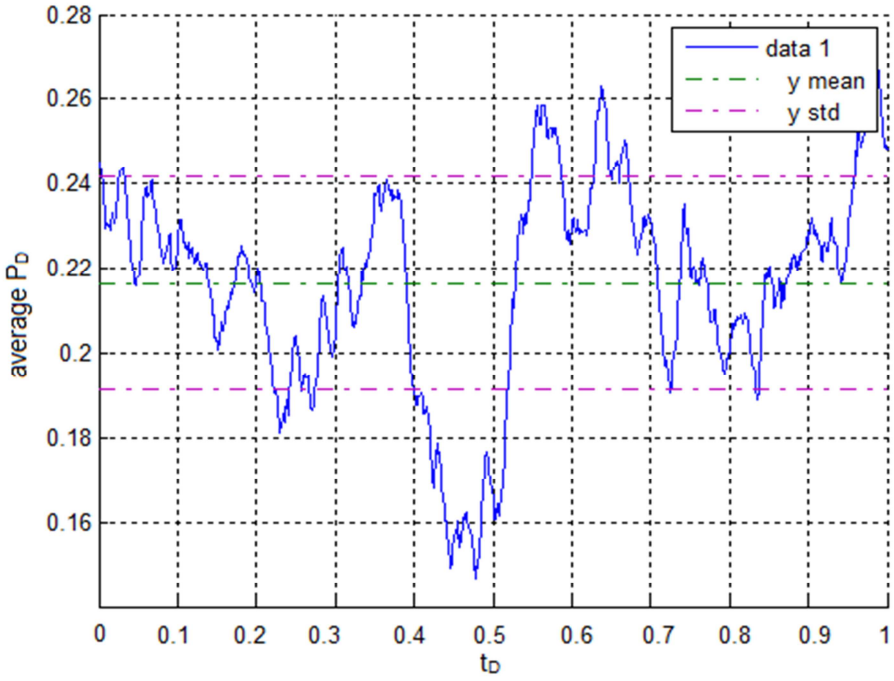

Figure 16. Continuation of passage of remaining bubbles from Figure 15: mean=0.2165; stdev.=0.02502 Δt_D=0.001; F_{dc}=0.

5.2 No Convection

The case without convection could reflect a cessation of gas flow on the large scale or immobilization of a bubble train, as suggested above. When a certain path is blocked by too-large a capillary resistance to flow, a new one may open, as observed experimentally by Falls et al. (8). In the abandoned path the lamellae then move only by diffusion.

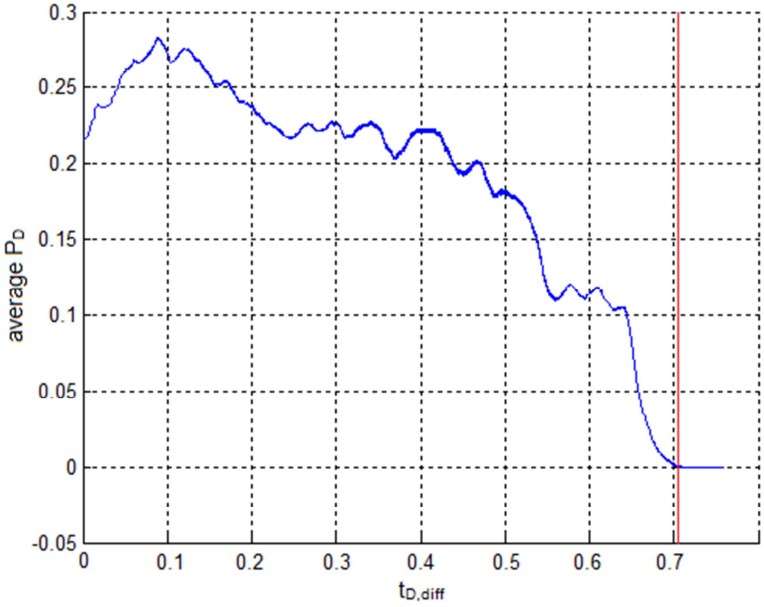

Figure 17. Evolution of average P_D for a train of bubbles initially smaller than pores, with no imposed convection: $\Delta t_{D,diff}$=0.0002. 100 bubbles merged, from those 24 merged due to the initial placement. The red line ($t_{D,diff}$ ~ 0.703) marks where $\Delta t_{D,diff}$ decreases to allow the lamellae to converge to the pore throat.

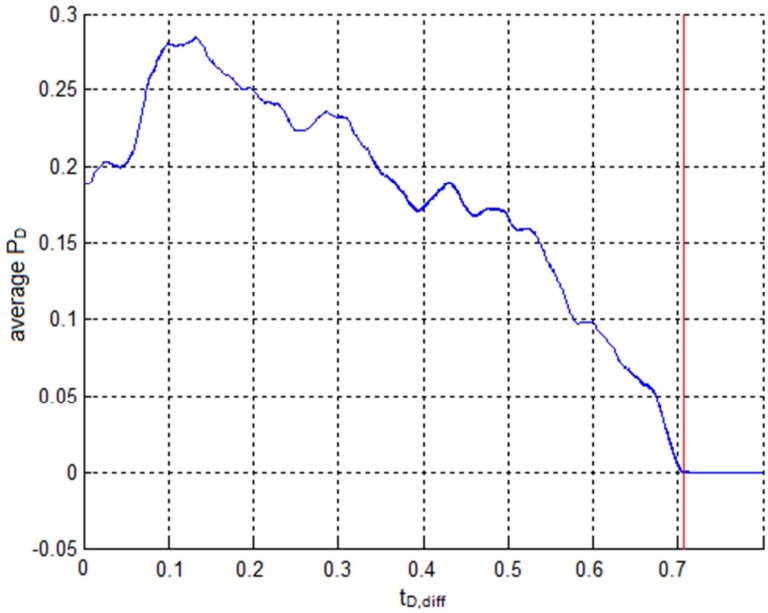

Figure 18. Evolution of population-average P_D for a train of bubbles larger than pores, with no imposed convection: $\Delta t_{D,diff}$=0.0002. The red line marks ($t_{D,diff}$ ~ 0.705) where $\Delta t_{D,diff}$ decreases to allow the lamellae to converge to the pore throat.

Figure 17 shows the evolution of average P_D for bubbles initially smaller than pores. Overall, population-average P_D initially increases, as lamellae in Interval 2 retreat toward the upstream throat where curvature is great. The trend is opposed by lamellae in Interval 4 approaching the downstream throat, but there are fewer of these. Then P_D decreases as more lamellae move toward the center of the throat, where P_D is zero. The population-average P_D fluctuates a somewhat over time. This partly reflects the major impact the positions of a few lamella can have: just five lamellae at maximum curvature instead of zero curvature (reflecting a slight

change in bubble volume) raises the population-average P_D of 300 bubbles by 0.02. Partly the fluctuation reflects the numerical artifact of using a finite time step. As lamellae approach the center of the throat they start oscillating in consecutive time steps, because the volume in Intervals 1 and 5 is so small but the changes in curvature large. For this reason we decreased the dimensionless time step late in the diffusion process (at the red line in Figure 17 and 18). We use Eq. 5.2-1 in the model to determine from where the diffusion step should decrease, together with additional statements for where and when it should apply (Appendix B, **%% incr/decr Vrt**).

$$|average\ P_D(i-1)| \leq |average\ P_D(i)| + 0.001 \qquad [5.2\text{-}1]$$

For this case, there are 300 bubbles initially but only 150 pore throats, since initial average bubble volume is ½ pore volume. One expects then half the lamellae to disappear. Instead, only 100 lamellae disappeared and even 24 of those where due to their initial placement. The reason is that about 20% of the lamellae (Fig. 13), or about 60 in total, are initially in Interval 3, with zero curvature; these lamellae do not respond to diffusion. For the 3D shapes computed by Cox et al. (Appendix A), all lamellae would approach pore throats and half the lamellae would disappear.

Figure 18 shows that when bubbles are larger than pores the lamellae again move to pore throats (except for those in Interval 3) but none disappear in throats because lamellae are not approaching the same throats. There are again small fluctuations in the average P_D, but smaller than the fluctuations in Figure 17. The reason for this can be found in the fact that Figure 17 has fewer bubbles to contribute to the average P_D and will therefore react more to the changes of one lamella. Using the cases of the super critical CO_2, CO_2 and N_2 foams in Section 4.2, one unit of dimensionless time in this case corresponds to about 0.026 s, $8.5*10^{-5}$ and 0.041 s for the three cases: the process up until $t_{D,diff} = 0.7$ shown in Figures 17 or 18 would take about 91 s, 0.30 s and 143.5 s, respectively. Within a matter of seconds or a few minutes, the lamellae would seek out and occupy pore throats.

5.3 Convection after only diffusion

Figures 19 and 20 illustrate the average capillary resistance to movement after a period of diffusion with no convection. Here the ratio of characteristic diffusion to convection rates F_{dc} is 0.2. One might expect a train of identical bubbles moving through identical pores, but the process is complicated by the fact that about 20% of the lamellae initially present are still at a variety of positions in Interval 3. (The fraction of lamellae starting in Interval 3 is larger for bubbles initially smaller than pores, because many of the other lamellae disappeared during the period of diffusion.) The flow rate of gas in this case is the same as in Figures 14 to 16 (the pistons upstream and downstream of the train move at the same velocity), but the lamellae move more slowly. Each lamella spends most of its time bulging forward, leaking gas to the upstream bubble, and therefore advancing more slowly than do the pistons.

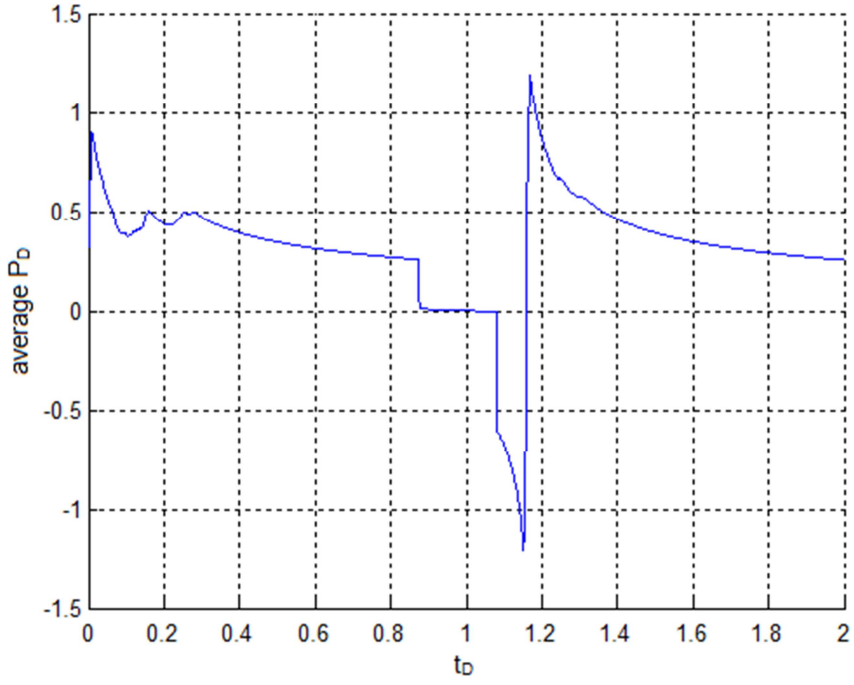

Figure 19. Reactivation of convection for bubbles smaller than pores (Figure 17): Δt_D=0.001; F_{dc}=0.2. Also 49 additional bubbles merged in this period, this adds up to 149 merged bubbles; bubbles cross more than 1 pore in the period of the plot.

Bubbles still merge in the process depicted in Figure 19, as closely-spaced lamellae initially in interval 3 intersect each other as the forward lamella jumps from Interval 3 to Interval 4. After crossing the first pore, the progress of the lamellae is exactly the same for each subsequent pore.

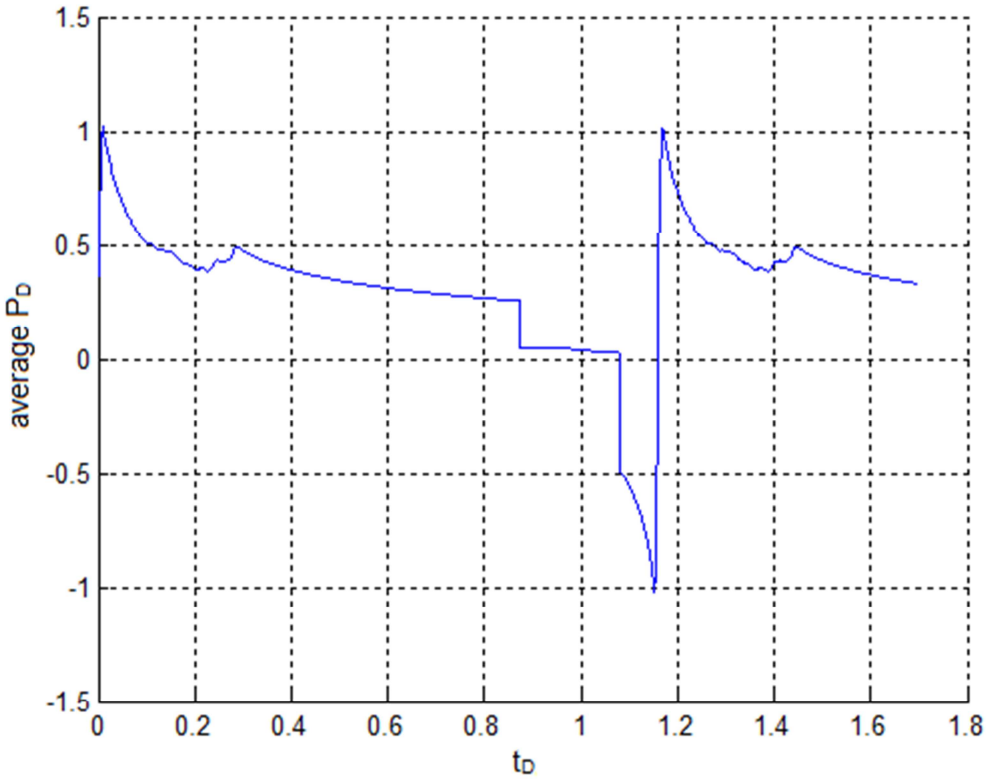

Figure 20. Reactivation of convection for bubbles larger than pores: Δt_D=0.001; F_{dc}=0.2. Bubbles cross more than 1 pore in the period of the plot.

The progress is similar for bubbles larger than pores (Figure 20), except that no lamellae merge and the passage is identical for each passage through one pore, directly from the start. Since all lamellae start in pore throats and reach the point of maximum curvature simultaneously, the maximum pressure different required to start the train going is almost 4½ times that required to keep a train of randomly positioned lamellae going in the absence of diffusion (Figure 14).

5.4 Convection and diffusion

When both convection and diffusion are active, we distinguish three cases, namely convection greater, the same or smaller than the nominal diffusion rate (F_{dc} <1, F_{dc} = 1, F_{dc} > 1).

When convection is greater than the characteristic diffusion rate, the bubbles cross each pore but spend more time in Intervals 1 and 2 in comparison with Intervals 4 and 5. Diffusion works against convection in Intervals 1 and 2 and with convection in Intervals 4 and 5. Therefore the population-average P_D is larger than in Figure 14.

The following graphs present a series of cases with F_{dc} < 1, with F_{dc} decreasing in the sequence.

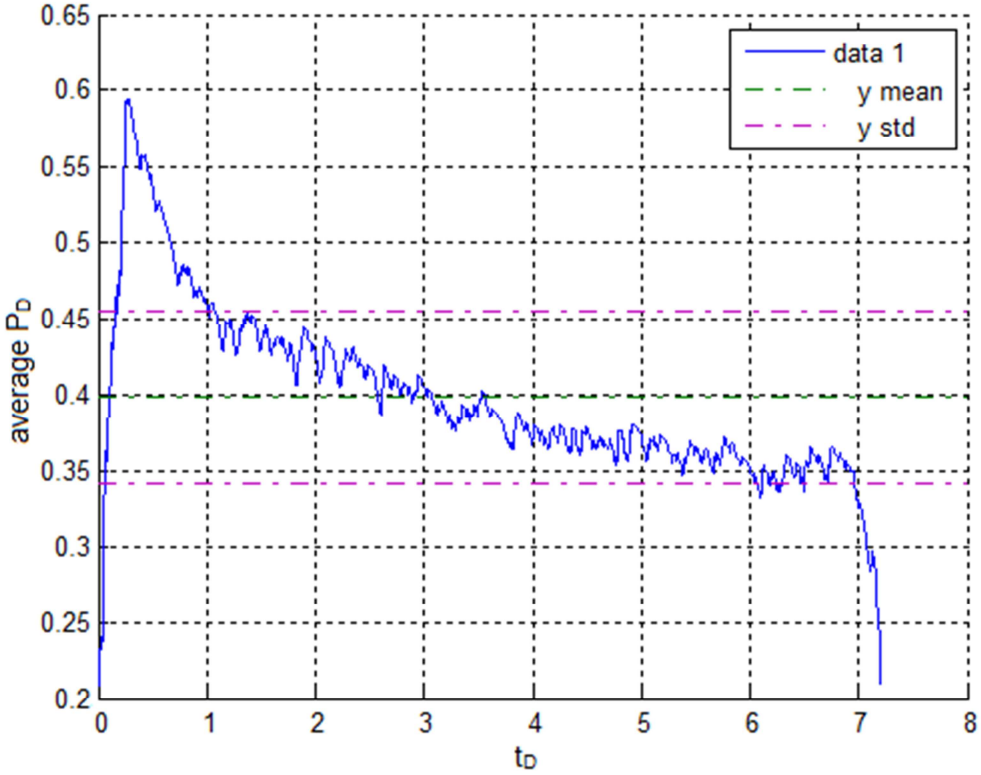

Figure 21. Convection just a little greater than diffusion: mean=0.3978; stdev.=0.05694 Δt_D=0.001; F_{dc}=0.9. The train has moved one pore length at t_D = 7.205.

In Figure 21, the original positions of the lamellae are randomly assigned, but this distribution is actually not typical of the case where diffusion is so significant. Lamellae cross Intervals 1 and 2 only slowly but rush through Intervals 4 and 5, since both diffusion and convection act together there. The population-average P_D rises rapidly at first because the roughly 30% of the lamellae initially in intervals 3, 4 and 5 are pushed into interval 1 and 2, while at the same time the bubbles that began in Intervals 1 and 2 are released at a much slower rate. As the entire population of lamellae has advanced one pore length, it recaptures its original distribution of positions, with much smaller average P_D. It may be that an initial distribution of positions reflecting a uniform distribution of bubble volumes may not be appropriate for a foam with such a fast diffusion rate. As in other cases, the fluctuations in average P_D for the train reflect the large impact that relatively small numbers of lamellae can have on the average P_D of the train. Note that although it may seem the first point of the graph doesn't match the last one, this is due to the fact that there are 7205 points displayed in Figure 21 therefore the first points overlaps with the y-axis of the graph and are therefore not visible.

The population-average P_D in Figure 21 is about double that with no diffusion (Figure 14). In this case the volumetric flow rate of gas is unchanged but the pressure difference is increased; thus gas mobility is about half that of the case with no diffusion. Stated differently, with the same pressure gradient, gas flow rate would be about half that with no diffusion. Contrary to expectations, a large rate of diffusion, by itself, *reduces* gas mobility by increasing the time lamellae spend in positions of large capillary resistance to forward movement.

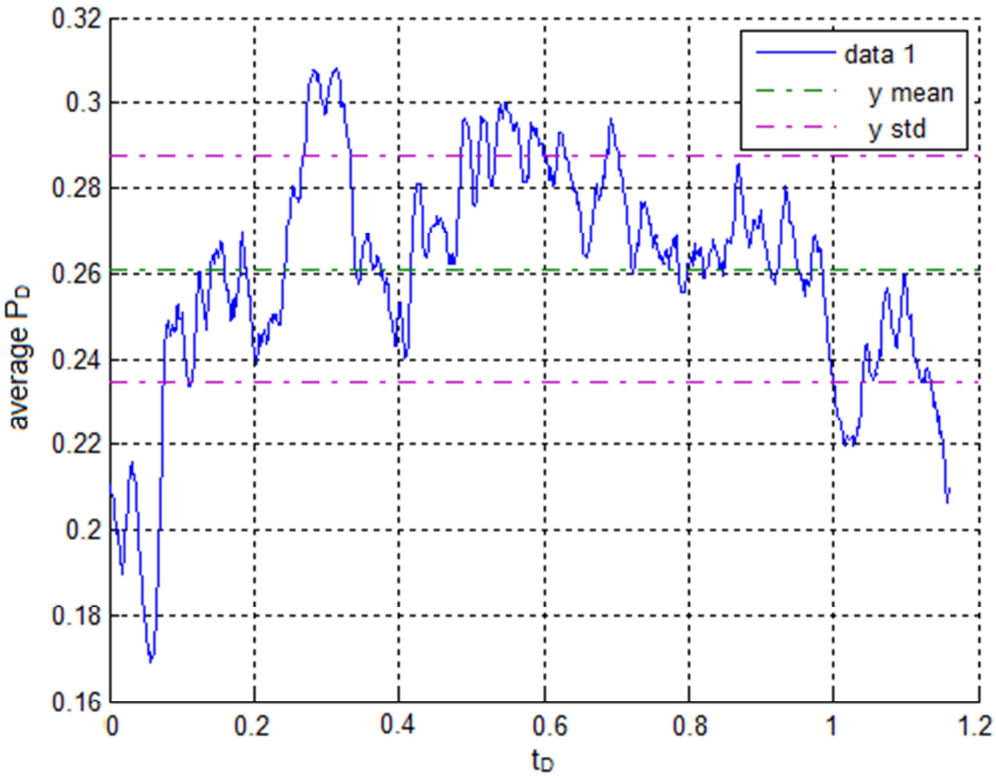

Figure 22. Convection significantly greater than diffusion: mean=0.2609; stdev.=0.02641; Δt_D=0.001; F_{dc}=0.2. The train has moved one pore length at t_D = 1.160.

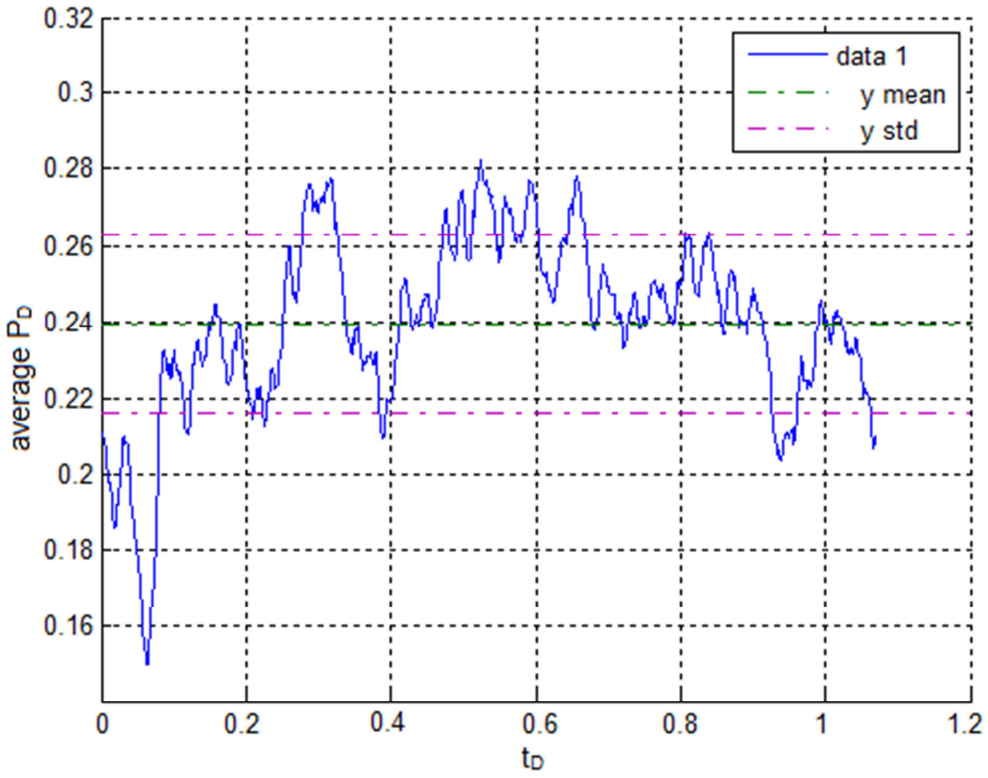

Figure 23. Convection significantly greater than diffusion: mean=0.2394; stdev.=0.02341; Δt_D=0.001; F_{dc}=0.1. The train has moved one pore length at t_D = 1.070.

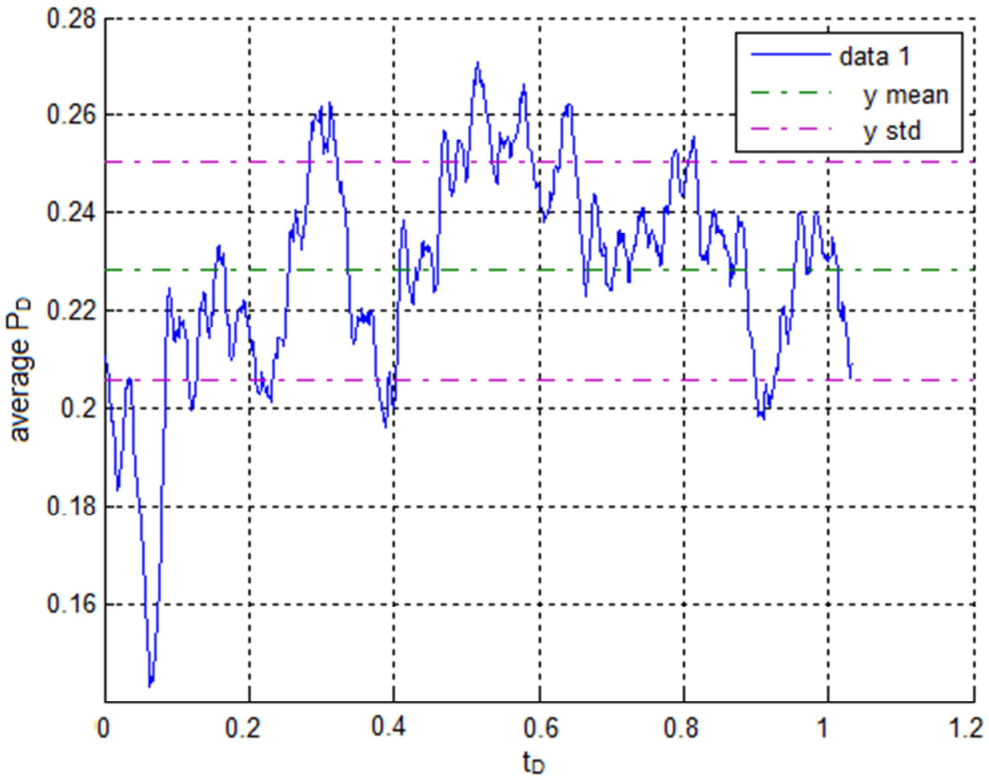

Figure 24. Convection significantly greater than diffusion: mean=0.2282; stdev.=0.02228; Δt_D=0.001; F_{dc}=0.05. The train has moved one pore length at t_D = 1.033.

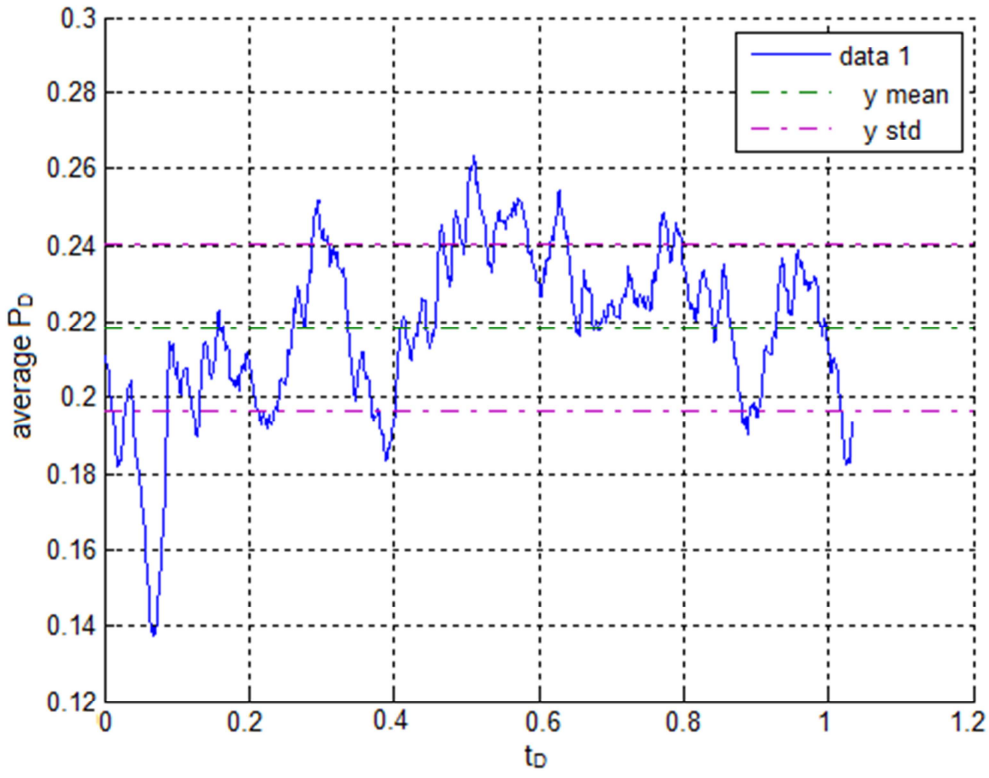

Figure 25. Convection significantly greater than diffusion: mean=0.2183; stdev.=0.0218 Δt_D=0.001; F_{dc}=0.01. The train has moved one pore length at t_D = 1.007.

From Figures 21 to 25 it can be seen that diffusion increases the population-average P_D. Comparing Figure 25 to Figure 14, when the characteristic diffusion rate is 1% of the convection rate it increases the average by capillary resistance to flow by about 0.8%. For F_{dc}=0.1 the population-average P_D rises by about 10.5%.

Our second case is F_{dc} = 1. In this case lamellae in interval 2 neither advance nor retreat; convection exactly balances diffusion there. All other lamella advance until they reach the start of Interval 2, where capillary resistance to flow is greatest. The distribution of P_D values eventually looks as in Figure 26, while the evolution of population-average P_D is shown in Figure 27.

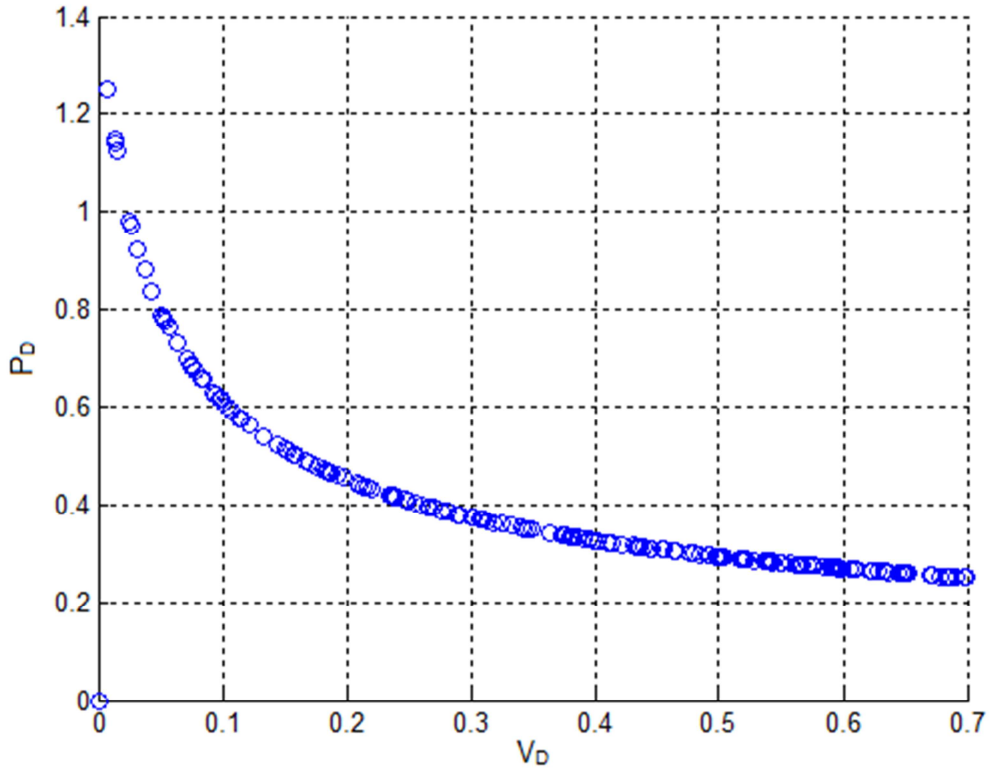

Figure 26. Convection just balanced with diffusion: final distribution of P_D and V_D values for F_{dc}=1. Bubbles initially in Interval 2 remain fixed in place, while all other bubbles, from Intervals 1, 3,4 and 5 move to the position of maximum value of P_D. Although only one open symbol is shown there, about 30% of the bubbles are at the maximum P_D, near the pore throat.

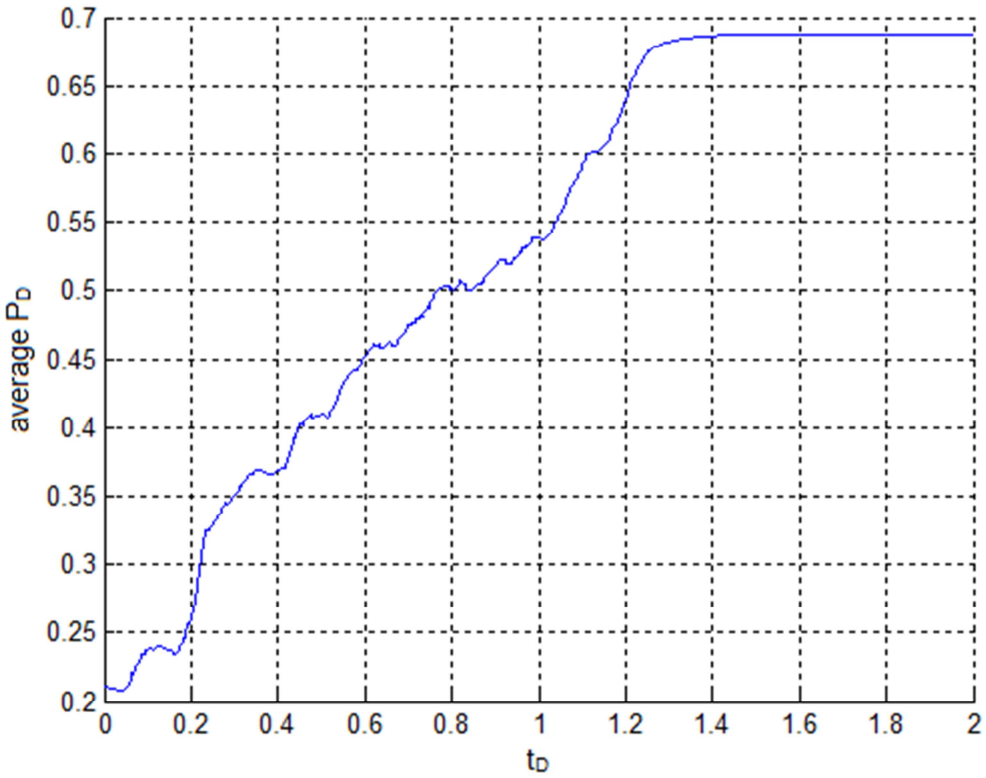

Figure 27. Convection just balanced with diffusion: evolution of population-average P_D. Δt_D=0.0002; F_{dc}=1. Lamellae in Interval 2 remain fixed, while all other lamellae advance to the position of maximum curvature, at the start of Interval 2.

The final value of P_D in Figure 27 can be estimated using the fact that in a randomly generated bubble size distribution about 70% of the lamellae (0.7*300=210) are in interval 2 with an average P_D of ~0.45 (Figure 9). These lamellae do not move, since diffusion and convection just balance in this interval. Therefore about 30% of the lamellae (0.3*300=90) move from their initial position to the maximum P_D at the start of interval 2: the value of P_D there is 1.2494. The population-average P_D for this case is estimated as (210*0.45+90*1.2494)/300=0.6898. As can be seen this is a good estimate of the final value.

Our final case is F_{dc} > 1: convection smaller than diffusion. In this case all lamellae become trapped in Interval 1. The finite rate of convection drives lamellae forward through Interval 3, while in Interval 2 diffusion pulls lamellae back until diffusion again balances convection in Interval 1. Diffusion pulls lamellae rapidly forward through Intervals 4 and 5. There is a unique position in Interval 1 where diffusion balances convection given by the position satisfying (cf. Eqs. 3.2-2 and 3.2-11)

$$P_D = \frac{\left(\frac{2R_t}{R_{t,0}}\right)}{F_{dc}} = \frac{1.2494}{F_{dc}} \qquad [5.4\text{-}1]$$

for our geometrical parameters.

All transport of gas is by diffusion in this case; although lamellae do not move, there is still a pressure difference arising from the static curvatures of all lamellae. Indeed, this pressure difference is required to drive the diffusion. Itamura and Udell (14) proposed such a mechanism for gas transport in foam in the context of steam foam (where condensation/evaporation, not diffusion, accounts for transport of steam across lamellae). Figure 28 shows the evolution of population-average P_D for F_{dc} = 2, Figure 29 for F_{dc} = 4 and Figure 30 for F_{dc} = 10. Eq. 5.4-1 is satisfied in all cases; the predicted values are 0.625, 0.312 and 0.125. Note that for diffusion faster than convection, the pressure difference required for a given rate of gas transport decreases with increasing rate of diffusion.

The average P_D increases at first and then decreases in Figures 28 and 29 because the last lamellae that reach the final position are the lamellae from interval 2. Those move backward to the pore throat and pass through the position of maximum curvature before reaching their final position. In Figure 30 the average P_D first increases then decreases and then increases again before it reaches its final value. This can be explained due to the fact that the lamellae from phase 3 who arrive later at the pore throat than the curved lamellae from interval 2 at the pore body.

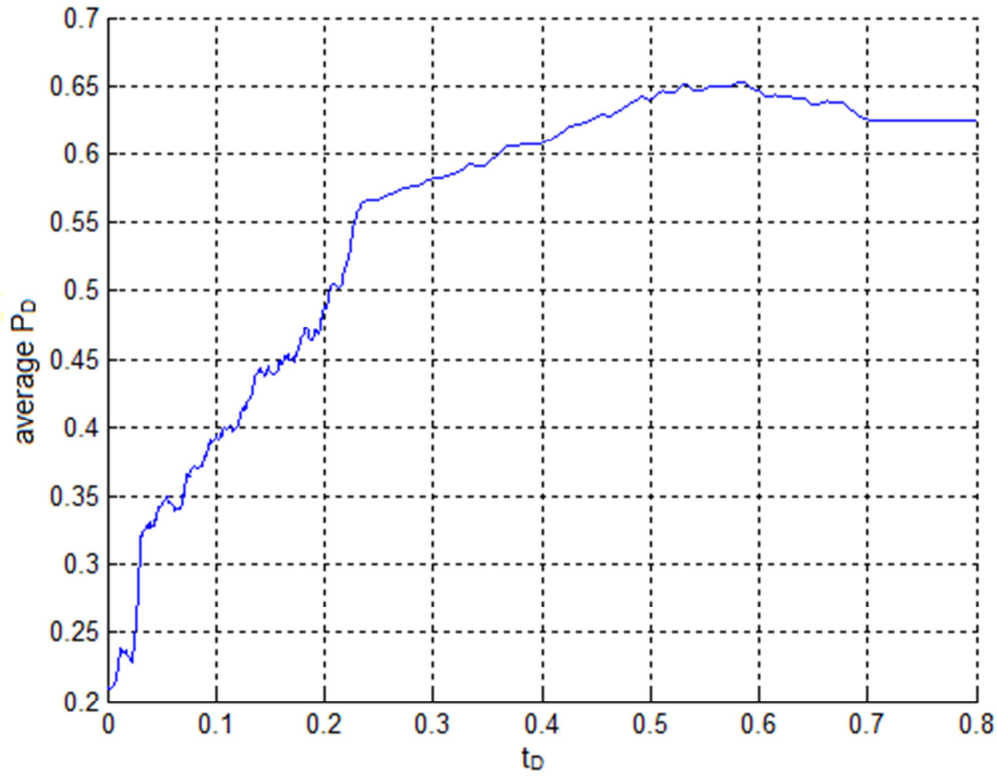

Figure 28. Diffusion faster than convection: Δt_D=0.0001; F_{dc}=2; bubbles bigger than pores.

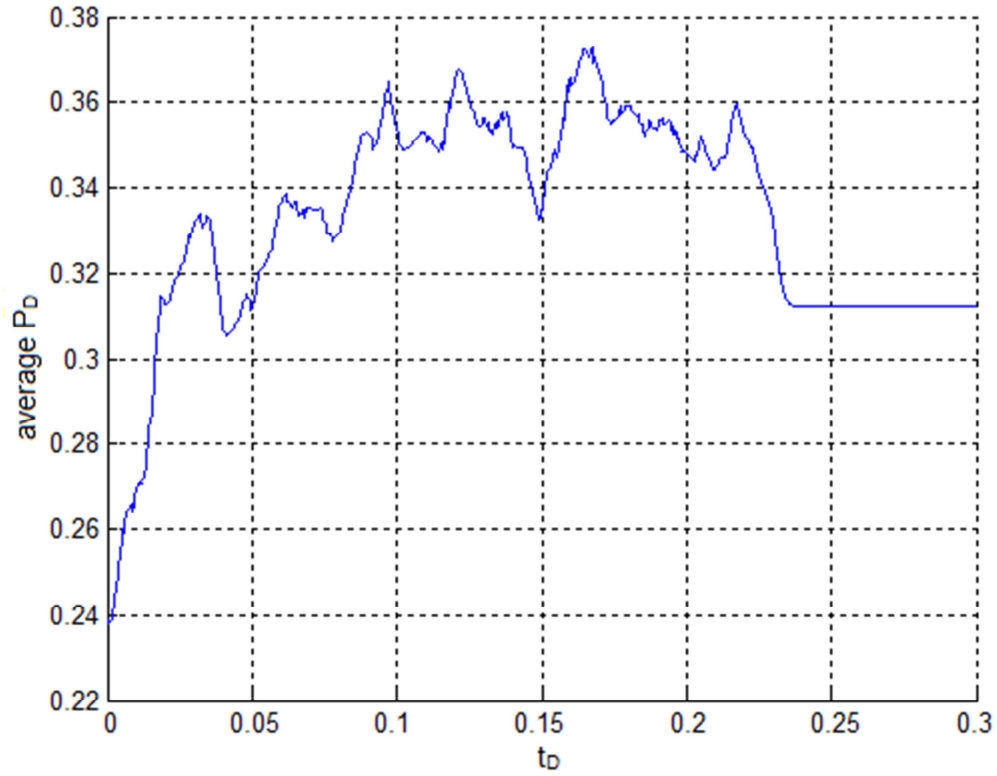

Figure 29. Diffusion faster than convection: Δt_D=0.0001; F_{dc}=4; bubbles bigger than pores.

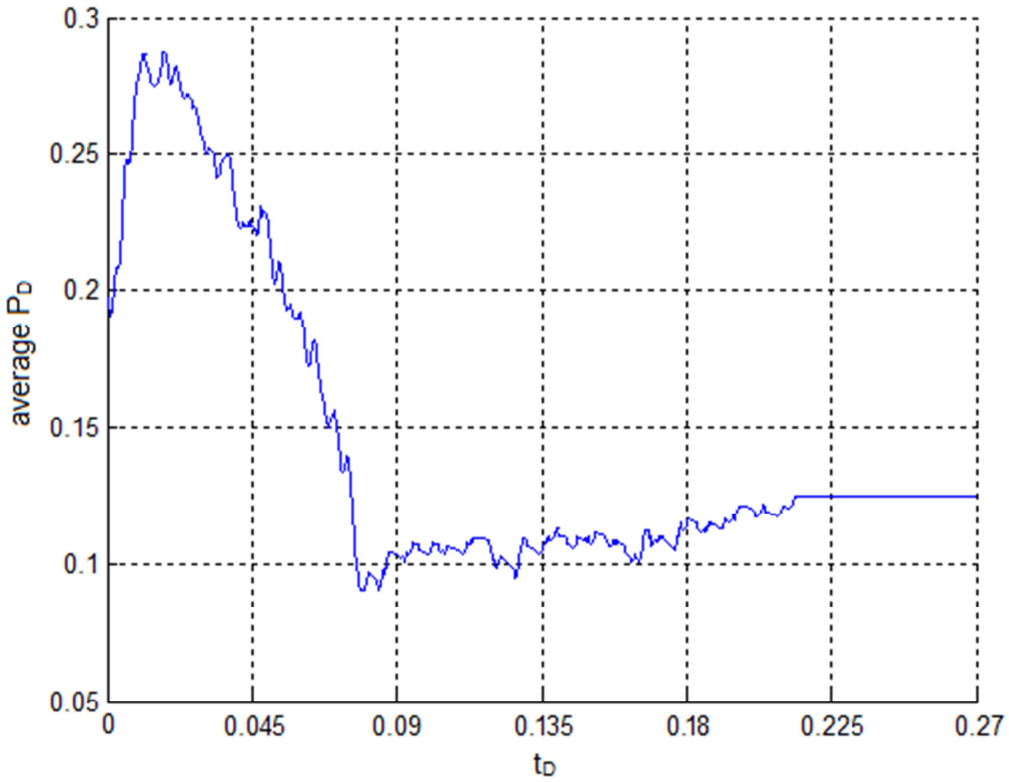

Figure 30. Diffusion faster than convection: Δt_D=0.00009; F_{dc}=10; bubbles bigger than pores.

6 Conclusions and discussion

In the previous sections the results from the 2D model are shown for the different ratios between the two driving forces for gas transport: convection of bubbles and diffusion through lamellae.

6.1 Conclusions

The results in the previous chapter show that even when the characteristic diffusion rate is 100 times slower than the convection rate, diffusion increases the average P_D. In fact for small values of F_{dc} the effect is nearly linear. This is presented in Figure 31 for bubbles larger than pores.

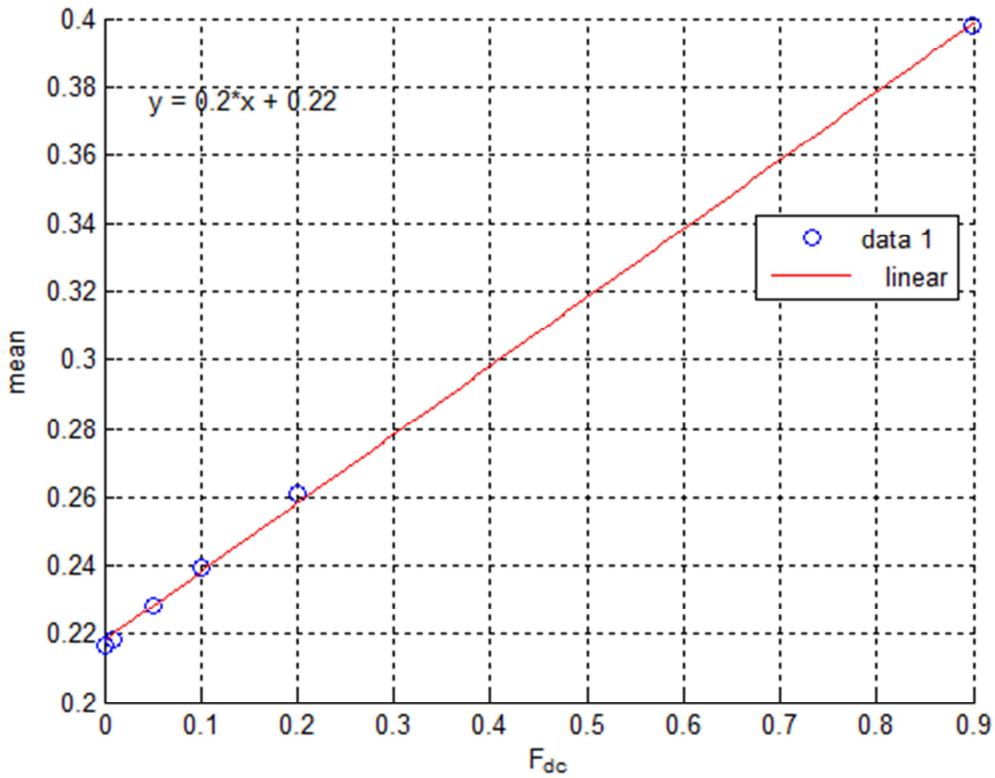

Figure 31. Population-average P_D as a function of F_{dc}, for $F_{dc} < 1$.

When the characteristic diffusion rate is greater than the convection rate ($F_{dc} > 1$), in our simple 2D model, lamellae become fixed at a certain position in the pore throats and we have an analytical formula for pressure difference across all lamellae Eq. 5.4-1. For $F_{dc} = 1$, lamellae in Interval 2 become fixed at their initial positions. For F_{dc} even slightly greater than 1 this anomaly disappears; therefore the trend of P_D v. F_{dc} has a break at $F_{dc} = 1$, as shown in Figure 32. For F_{dc} just slightly greater than one, according to Eq. 5.4-1, $P_D = 1.2497$, not 0.69. For $F_{dc} > 1$, P_D is inversely proportional to diffusion rate.

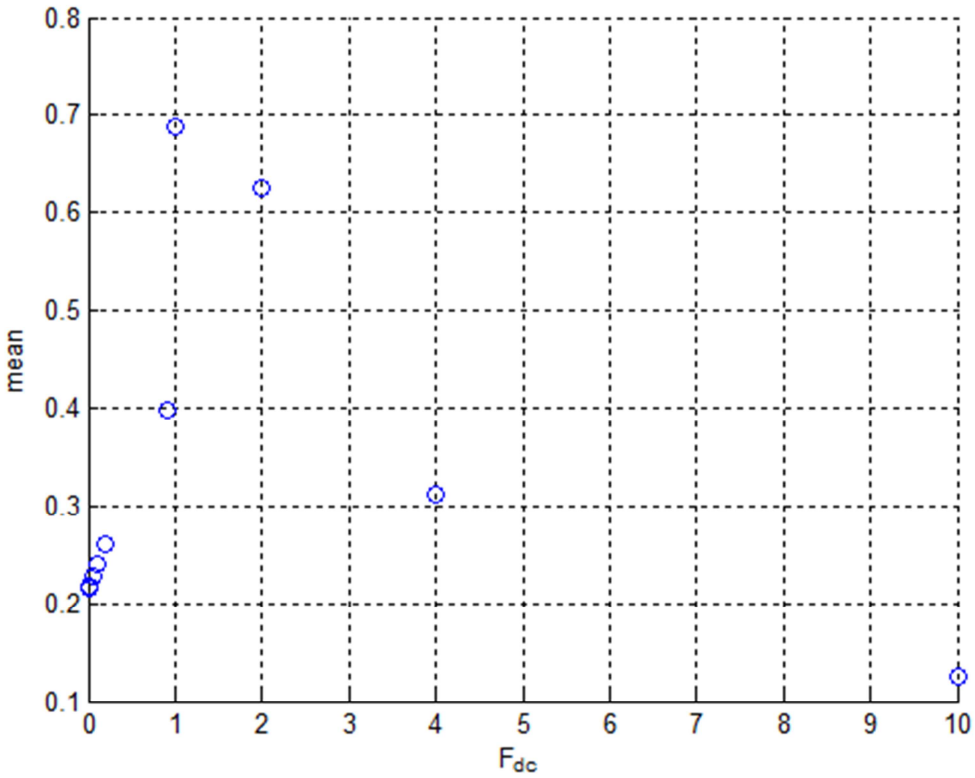

Figure 32. Population-average P_D as a function of F_{dc} over the entire range examined in this thesis.

When the bubbles are smaller than the pores, with multiple lamellae in one pore, some will merge and therefore affect the bubble size distribution. Merging occurs either as lamellae cross at jumps, by overlap of Plateau borders, or by diffusion as multiple lamellae move toward the same pore throat. In our results, merging due to lamellae converging on the same throat occurred only for $F_{dc} > 1$. (In the study of Cohen et al., (11), where this mechanism dominates, there is no imposed convection.) When $F_{dc} < 1$, the lamellae only merge at the pore body as they jump to a next interval and when the bubbles are smaller than the pores. In our study, merging affects the bubble-size distribution primarily as lamellae jump at pore bodies, one bubble becomes isolated and bypassed, and subsequently disappears by diffusion.

6.2 Discussion

Although this 2D model is nice to get an idea for what will happen with the average P_D as F_{dc} changes, this is still only to get an idea. Since in situ even the bubbles bigger than pores won't be safe from merging as multiple pores are connected to each other, this will influence the BSD and that will in turn affect the average P_D.

Also a change in the model to allow different pore sizes and volumes would be interesting to see, since bubbles will have different velocities from pore to pore, and are therefore possibly allowed to creep up to each other.

6.3 Acknowledgement

I do like to thank professor Rossen at the TU Delft for making this project possible for me, and all his support and ideas in the process.

Bibliography

1. Rossen, W.R., "Foams in Enhanced Oil Recovery," in R. K. Prud'homme and S. Khan, ed., *Foams: Theory, Measurements and Applications*, Marcel Dekker, New York, pp. 413-464 (1996).

2. Alvarez, J. M., Rivas, H., and Rossen, W.R., "A Unified Model for Steady-State Foam Behavior at High and Low Foam Qualities," *SPE Journal* **6**, 325-333 (Sept. 2001).

3. Xu, Q., and Rossen, W. R., "Effective Viscosity of Foam in Periodically Constricted Tubes," *Colloids Surfaces A: Physicochem Eng. Aspects* **216** (1-3), 175-194 (2003).

4. Rossen, W.R, "Theory of Mobilization Pressure Gradient of Flowing Foams in Porous Media. I. Incompressible Foam", J. Colloid Interface Sci. 136, 1-16 (1990).

5. Rossen, W.R, "Theory of Mobilization Pressure Gradient of Flowing Foams in Porous Media. II. Effect of Compressibility," J. Colloid Interface Sci. 136, 17-37 (1990).

6. Rossen, W.R, "Theory of Mobilization Pressure Gradient of Flowing Foams in Porous Media. III Asymmetric Lamella Shapes," J. Colloid Interface Sci. 136, 38-53 (1990).

7. Rossen, W.R, "Minimum Pressure Gradient for Foam Flow in Porous Media: Effect of Interactions with Stationary Lamellae," J. Colloid Interface Sci. 139, 457-468 (1990).

8. Falls, A.H., Musters, J.J., Ratulowski, J., "The Apparent Viscosity of Foams in Homogeneous Bead Packs," SPE 16048, 155-164 (1989).

9. Cox, S.J., Neethling, S., Rossen, W.R., Schleifenbaum, W., Schmidt-Wellenburg, P., and Cilliers, J.J., "A Theory of the Effective Yield Stress of Foam in Porous Media: the motion of a soap film traversing a three-dimensional pore," Colloids Surfaces A: Physicochem Eng. Aspects 245, 143-151 (2004).

10. Farajzadeh, R., Muruganathan, R.M., Krastev, R., Rossen, W.R., "Effect of gas type on foam film permeability and its implications for foam flow in porous media," SPE 131297 presented at the SPE EUROPEC/EAGE Annual Conference and Exhibition held in Barcelona, Spain,14-17 June 2010.

11. Cohen, D., Patzek, T.W., Radke, C.J., "Two-Dimensional Network Simulation of Diffusion-Driven Coarsening of Foam Inside a Porous Medium," J. Colloid Interface sci. 179, 357-373 (1996).

12. CRC Standard Mathematical Tables, editor, W.H. Beyer, CRC Press INC., 1984, 27th Edition.

13. Kil, R. A., Nguyen, Q. P., and Rossen, W. R., "Determining Trapped Gas in Foam From CT Images," *SPE Journal* **16**, 24-34 (2011).

14. Itamura, M. T., and Udell, K. S., "The Role of Noncondensible Gases in Heat and Mass Transfer in Porous Media Containing a Steam Foam", *Multiphase Flow, Heat and Mass Transfer*, ASME HTD **109**, 87-92 (1989).

Appendix A. 3D calculations of Cox et al. (9)

Cox et al. (9) calculated P_D v. dimensionless volume for a variety of 2D and 3D pore shapes using the Surface Evolver. We reproduce two examples below.

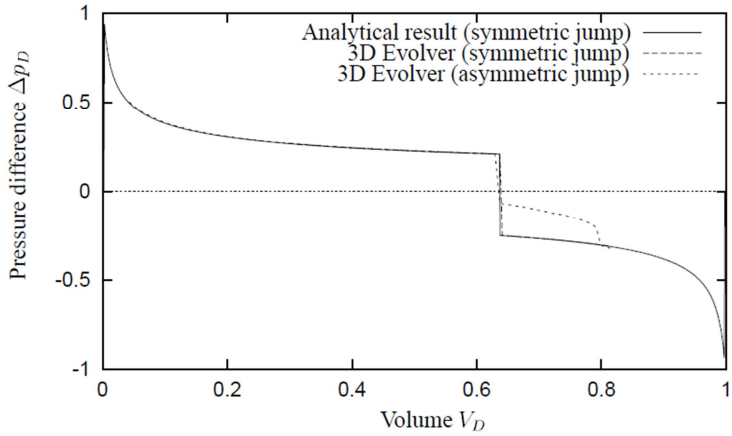

Figure A1. Dimensionless pressure difference (called her Δp_D) v. dimensionless volumetric position in pore for 3D biconical pores, from Cox et al. (9). Cases denoted "symmetric jump" were constrained not to allow the asymmetric jump that would occur spontaneously in either 2D or 3D. With the asymmetric jump allowed, Δp_D is less than zero for all of Interval 3.

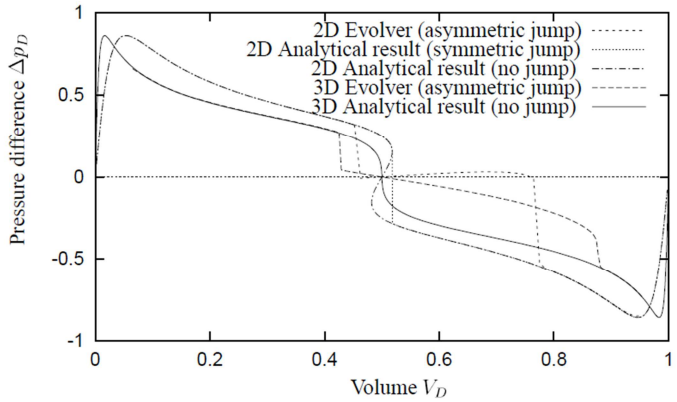

Figure A2. Dimensionless pressure difference v. dimensionless volumetric position in pore for 2D and 3D sinusoidal pores, from Cox et al. (9). Cases denoted "symmetric jump" were constrained not to allow the asymmetric jump that would occur spontaneously in either 2D or 3D. For the 3D case allowing for the asymmetric jump ("3D Evolver"), Δp_D decreases monotonically in Interval 3.

In principle one could use these results to repeat our 2D calculations for 3D lamella shapes. One can infer diffusive flux through lamellae using the curvatures implied by Δp_D in these plots. Unfortunately, Cox et al. (9) do not record lamella areas from their calculations, which is required to compute diffusive fluxes (Eq. 3.2-1). For symmetric lamellae, with spherical shape, this calculation of area is straight-forward, but not for the complex 3D asymmetric shapes.

As noted in the text, in the absence of convection, in both 3D pore shapes, lamellae in Interval 3 would diffuse either backwards to the upstream throat or downstream to the next throat; no lamellae would be stranded in Interval 3 as in our 2D model. In the 2D sinusoidal pore, however, lamellae in Interval 3 would diffuse backward or forward to a dimensionless position of about 0.5, with zero pressure difference, as in our model.

Appendix B: Calculation method

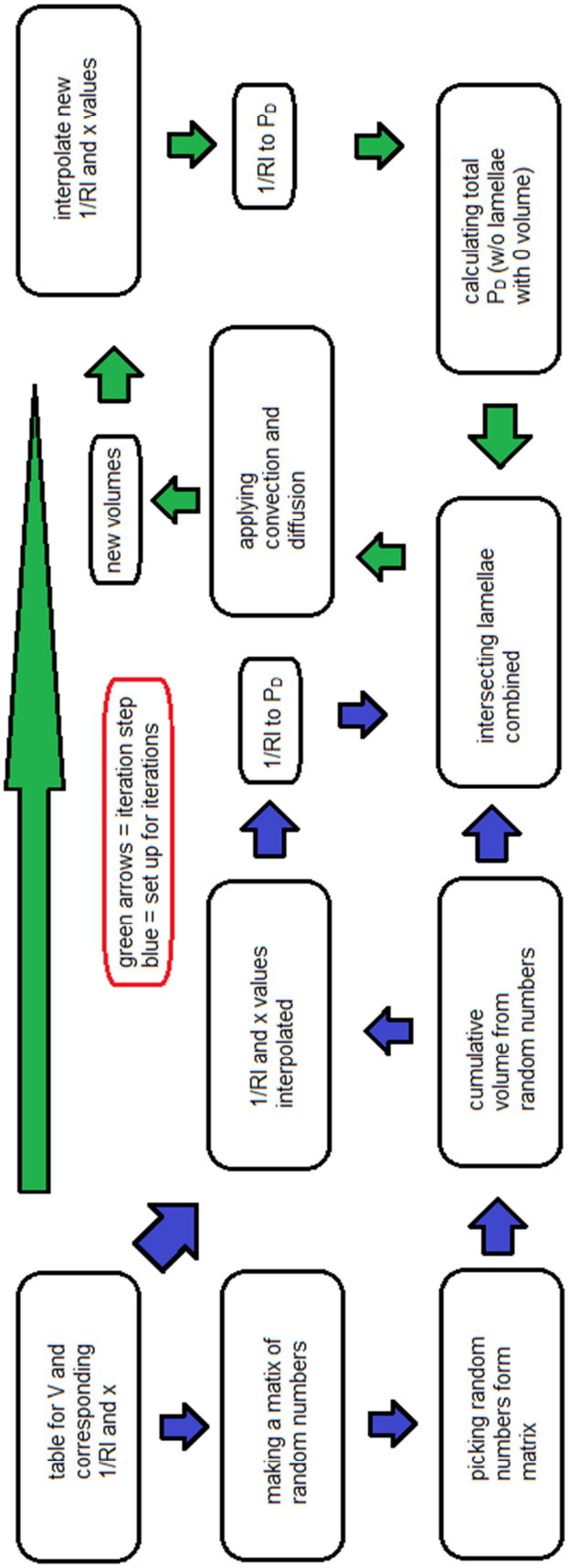

Figure B1. Flow chart for the calculation method for the advance of lamellae

The model initially contained 2 more situations for the pore shape. These can still be made by this model, but are not threaded in this thesis as the lamella does things in interval 3 that need more investigation.

```
%% Volume 2D pore
clear all; clc
%% parameter meaning
% beta(b); largest angle >= 90 degree
% alfa(a); alfa=180-beta
% theta(t); theta=0.5*alfa=90-0.5*beta
% C1; diffusion constant
% C2; convection constant
% Rt; radius pore throat
% Rb; radius pore body
% Rl; 1/radius lamella
% Rlmax; maximum radius lamella
% Rl0; minimum radius lamella
% L; Length pore
% T; dimensionless angle
% RhoT (RT); 2*Rt/L
% RhoB (RB); 2*Rb/L
% RhoB-RhoT<=1
% Vtot; total volume
% V##; volume in a situation at a certain angle theta at a certain place x
% V#; dimensionless volume in a situation at a certain angle theta at a
certain place x
% V##max; maximum volume in a certain situation
% Vrb#; volume of a random bubble
% x#; x for a certain situation
% xL; dimensionless length
% Pd; dimensionless pressure, Pd=2*Rt/Rl

%% parameters values

clear all;
% example parameters
% b=90;                          ;95
% a=180-b;
% t=90-0.5*b;
% Rt=1;                          ;1
% Rb=3;                          ;6
% L=2*((Rb-Rt)*tand(0.5*b));
%
% and
%
% b=120;
% a=180-b;
% t=90-0.5*b;
% Rt=1;
% Rb=4;
% L=2*((Rb-Rt)*tand(0.5*b));

Rt=10*10^-6;                    % 10um            % RB-RT<=1 see "check"
Rb=50*10^-6;                   % 125um
L=100*10^-6;
b=2*((180*atan((0.5*L)/(Rb-Rt)))/pi);                              %120     %
larger or equal than 90
a=180-b;
t=90-0.5*b;
Rl0=Rt/sind(t);
Rlmax=Rl0+((0.5*L)/cosd(t));
Vtot=2*(Rb*Rlmax*cosd(t))-2*(Rt*Rl0*cosd(t));
```

```
RB=2*Rb/L;
RT=2*Rt/L;
check=RB-RT;    %should be smaller or equal to 1

%% situation a) angel theta increases from 0 to 90-0.5*beta

t0=linspace(0,t,100);
Va=zeros(length(t0),1);
for i=1:length(t0);
    Va(i,1)=0.5*(Rl0)^2*(2*(t0(1,i)*pi/180)-sind(2*t0(1,i)));
end

Vamax=0.5*(Rl0)^2*(2*(t*pi/180)-sind(2*t));
V1=Va/Vtot;
T0=t0/t;
k1=(2*(t0*pi/180)-sind(2*t0));
Rl1=sqrt((2*Vamax)*k1.^-1);
Rla=Rl1'.^-1;
xL0=zeros(1,length(t0));

%% situation b) x goes from 0 to 0.5*L

xb=linspace(0,0.5*L,400);
Vab=zeros(length(xb),1);
for i=1:length(xb);
    Vab(i,1)=Vamax+(((t*pi)/180)*((Rt/sind(t)+(xb(1,i))/cosd(t))^2-
(Rt/sind(t))^2));
end

Vabmax=Vamax+(((t*pi)/180)*((Rt/sind(t)+(0.5*L)/cosd(t))^2-
(Rt/sind(t))^2));
V2=Vab/Vtot;
xL1=xb/L;
Rl2=(Rt/sind(t)+xb/cosd(t));
Rlb=Rl2'.^-1;

%% situation c) lamella jumps to a new x with same Vabmax at first

if cosd(2*t)*Rlmax<=Rl0;
    % new surface calculated with a small triangle and 2 rectangles of
    % which the largest one is increasing
    % at the moment it seems this calculation is not needed since the
    % maximum this surface can acquire is smaller than Vabmax
    x1=(((Vabmax-Rt*Rl0*cosd(t)-(Rl0*(Rlmax-
Rl0)))/Rlmax)+Rl0)*cosd(t)+0.5*L;
    xc1=linspace(x1,L,400);
    Vc1=zeros(length(xc1),1);
    for i=1:length(xc1);
        Vc1(i,1)=(Rt*Rl0*cosd(t))+(Rl0*(Rlmax-Rl0))+(Rlmax*((xc1(1,i)-
0.5*L)/cosd(t)-Rl0));
    end

    Vc1max=(Rt*Rl0*cosd(t))+(Rl0*(Rlmax-Rl0))+(Rlmax*((L-0.5*L)/cosd(t)-
Rl0));
    V3=Vc1/Vtot;
    xL2=xc1/L;
    Rl3=inf(length(xc1),1);
    Rlc=Rl3.^-1;
    X=sind(t)*Rlmax;                          % used for crossing lamella
    % new surface calculated with a large triangle - the imaginary triangle
```

```
    % + an increasing rectangle
else x2=((Vabmax-(0.5*Rlmax^2*sind(2*t)*cosd(2*t)-
Rt*Rl0*cosd(t)))/(sind(2*t)*Rlmax))*cosd(t)+0.5*L;
    xc2=linspace(x2,0.5*L+(Rlmax-cosd(2*t)*Rlmax)*cosd(t),400);
    Vc2=zeros(length(xc2),1);
for i=1:length(xc2);
    Vc2(i,1)=(0.5*Rlmax^2*sind(2*t)*cosd(2*t)-
Rt*Rl0*cosd(t))+sind(2*t)*Rlmax*((xc2(1,i)-0.5*L)/cosd(t));
end

Vc2max=(0.5*Rlmax^2*sind(2*t)*cosd(2*t)-
Rt*Rl0*cosd(t))+sind(2*t)*Rlmax*(((0.5*L+(Rlmax-cosd(2*t)*Rlmax)*cosd(t))-
0.5*L)/cosd(t));
V3=Vc2/Vtot;
xL2=xc2/L;
Rl3=inf(length(xc2),1);
Rlc=Rl3.^-1;
X=(sind(t)*(sin(2*(t*pi/180))*Rlmax));          % used for crossing lamella
end

%% situation e) this is the inverse of situation b

if cosd(2*t)*Rlmax<=Rl0;
    if Vabmax>Vc1max
        x5=-1*((sqrt(((Vabmax-Vtot+Vamax)/(-t*pi/180))+Rl0^2)-Rl0)*cosd(t)-
L);
        xe1=linspace(x5,L,400);
        Ve1=zeros(length(xe1),1);
        for i=1:length(xe1);
            Ve1(i,1)=Vtot-Vamax-(t*pi/180)*((Rl0+(L-xe1(1,i))/cosd(t))^2-
Rl0^2);
        end
        Vemax=Vtot-Vamax-(t*pi/180)*((Rl0+(L-L)/cosd(t))^2-Rl0^2);
        V4=Ve1/Vtot;
        xL3=xe1/L;
        Rl4=-1*(Rt/sind(t)+(L-xe1)/cosd(t));
        Rld=Rl4'.^-1;

    else x5=-1*((sqrt(((Vc1max-Vtot+Vamax)/(-t*pi/180))+Rl0^2)-
Rl0)*cosd(t)-L);
        xe2=linspace(x5,L,400);
        Ve2=zeros(length(xe2),1);
        for i=1:length(xe2);
            Ve2(i,1)=Vtot-Vamax-(t*pi/180)*((Rl0+(L-xe2(1,i))/cosd(t))^2-
Rl0^2);
        end
        Vemax=Vtot-Vamax-(t*pi/180)*((Rl0+(L-L)/cosd(t))^2-Rl0^2);
        V4=Ve2/Vtot;
        xL3=xe2/L;
        Rl4=-1*(Rt/sind(t)+(L-xe2)/cosd(t));
        Rld=Rl4'.^-1;
    end
else x5=-1*((sqrt(((Vc2max-Vtot+Vamax)/(-t*pi/180))+Rl0^2)-Rl0)*cosd(t)-L);
xe3=linspace(x5,L,400);
Ve3=zeros(length(xe3),1);
for i=1:length(xe3);
    Ve3(i,1)=Vtot-Vamax-(t*pi/180)*((Rl0+(L-xe3(1,i))/cosd(t))^2-Rl0^2);
end
Vemax=Vtot-Vamax-(t*pi/180)*((Rl0+(L-L)/cosd(t))^2-Rl0^2);
V4=Ve3/Vtot;
xL3=xe3/L;
```

```
Rl4=-1*(Rt/sind(t)+(L-xe3)/cosd(t));
Rld=Rl4'.^-1;
end

%% situation g) angle theta decreases again till 0

t1=linspace(t,0,100);
Vg=zeros(length(t0),1);
for i=1:length(t1);
    Vg(i,1)=Vtot-0.5*(Rl0)^2*(2*(t1(1,i)*pi/180)-sind(2*t1(1,i)));
end

Vgmax=0.5*(Rl0)^2*(2*(t1(1,length(t1))*pi/180)-sind(2*t1(1,length(t1))));
V5=Vg/Vtot;
T1=t1/t;
k2=(2*(t1'*pi/180)-sind(2*t1'));
Rl5=-1*sqrt((-2*(Vemax-Vtot))*k2.^-1);
Rle=Rl5.^-1;
xL4=ones(1,length(t0));

%% dimension V, plotting

if cosd(2*t)*Rlmax<=Rl0
    if Vabmax>Vc1max
    V=[V1(1:99);V2;V4(2:399);V5];
    xL=[xL0(1:99)';xL1';xL3(2:399)';xL4'];

    figure; p=zeros(5,1);
    p(1)=subplot(5,1,1); hold on; grid on;
    plot(V);  title(' Volume vs data points');
    p(2)=subplot(5,1,2); hold on; grid on;
    plot(T0,V1);  title(' V1 vs angle');
    p(3)=subplot(5,1,3); hold on; grid on;
    plot(xL1,V2);  title(' V2 vs position');
    p(4)=subplot(5,1,4); hold on; grid on;
    plot(xL3,V4);   title(' V4 vs position');
    p(5)=subplot(5,1,5); hold on; grid on;
    plot(T1,V5);   title(' V5 vs angle'); set(gca,'XDir','reverse');

    else V=[V1(1:99);V2;V3(2:399);V4(1:399);V5];
            xL=[xL0(1:99)';xL1';xL2(2:399)';xL3(1:399)';xL4'];

            figure; p=zeros(6,1);
            p(1)=subplot(6,1,1); hold on; grid on;
            plot(V);  title(' Volume vs data points');
            p(2)=subplot(6,1,2); hold on; grid on;
            plot(T0,V1);  title(' V1 vs angle');
            p(3)=subplot(6,1,3); hold on; grid on;
            plot(xL1,V2);  title(' V2 vs position');
            p(4)=subplot(6,1,4); hold on; grid on;
            plot(xL2,V3);   title(' V3 vs position');
            p(5)=subplot(6,1,5); hold on; grid on;
            plot(xL3,V4);   title(' V4 vs position');
            p(6)=subplot(6,1,6); hold on; grid on;
            plot(T1,V5);   title(' V5 vs angle');
set(gca,'XDir','reverse');
    end
else V=[V1(1:99);V2;V3(2:399);V4(1:399);V5];
xL=[xL0(1:99)';xL1';xL2(2:399)';xL3(1:399)';xL4'];
```

```
figure; p=zeros(6,1);
p(1)=subplot(6,1,1); hold on; grid on;
plot(V);  title(' Volume vs data points');
p(2)=subplot(6,1,2); hold on; grid on;
plot(T0,V1);  title(' V1 vs angle');
p(3)=subplot(6,1,3); hold on; grid on;
plot(xL1,V2);  title(' V2 vs position');
p(4)=subplot(6,1,4); hold on; grid on;
plot(xL2,V3);   title(' V3 vs position');
p(5)=subplot(6,1,5); hold on; grid on;
plot(xL3,V4);   title(' V4 vs position');
p(6)=subplot(6,1,6); hold on; grid on;
plot(T1,V5);   title(' V5 vs angle'); set(gca,'XDir','reverse');
end

%% 1/Rl vs V

if cosd(2*t)*Rlmax<=Rl0
    if Vabmax>Vc1max
    Rl=[Rla(1:99);Rlb;Rld(2:399);Rle];
    figure; g=zeros(5,1);
    g(1)=subplot(5,1,1); hold on; grid on;
    plot(V,Rl); axis([0 1 -1 1]); title(' 1/Rl vs Volume');
    g(2)=subplot(5,1,2); hold on; grid on;
    plot(V1,Rla);  title(' 1/Rl1 vs V1');
    g(3)=subplot(5,1,3); hold on; grid on;
    plot(V2,Rlb);  title(' 1/Rl2 vs V2');
    g(4)=subplot(5,1,4); hold on; grid on;
    plot(V4,Rld);   title(' 1/Rl4 vs V4');
    g(5)=subplot(5,1,5); hold on; grid on;
    plot(V5,Rle);   title(' 1/Rl5 vs V5');

    else Rl=[Rla(1:99);Rlb;Rlc(2:399);Rld(1:399);Rle];
            figure; g=zeros(6,1);
            g(1)=subplot(6,1,1); hold on; grid on;
            plot(V,Rl); axis([0 1 -1 1]); title(' 1/Rl vs Volume');
            g(2)=subplot(6,1,2); hold on; grid on;
            plot(V1,Rla);  title(' 1/Rl1 vs V1');
            g(3)=subplot(6,1,3); hold on; grid on;
            plot(V2,Rlb);  title(' 1/Rl2 vs V2');
            g(4)=subplot(6,1,4); hold on; grid on;
            plot(V3,Rlc);   title(' 1/Rl3 vs V3');
            g(5)=subplot(6,1,5); hold on; grid on;
            plot(V4,Rld);   title(' 1/Rl4 vs V4');
            g(6)=subplot(6,1,6); hold on; grid on;
            plot(V5,Rle);   title(' 1/Rl5 vs V5');
    end
else Rl=[Rla(1:99);Rlb;Rlc(2:399);Rld(1:399);Rle];

    figure; g=zeros(6,1);
    g(1)=subplot(6,1,1); hold on; grid on;
    plot(V,Rl); axis([0 1 -1 1]); title(' 1/Rl vs Volume');
    g(2)=subplot(6,1,2); hold on; grid on;
    plot(V1,Rla);  title(' 1/Rl1 vs V1');
    g(3)=subplot(6,1,3); hold on; grid on;
    plot(V2,Rlb);  title(' 1/Rl2 vs V2');
    g(4)=subplot(6,1,4); hold on; grid on;
    plot(V3,Rlc);   title(' 1/Rl3 vs V3');
    g(5)=subplot(6,1,5); hold on; grid on;
    plot(V4,Rld);   title(' 1/Rl4 vs V4');
    g(6)=subplot(6,1,6); hold on; grid on;
```

```
    plot(V5,Rle);   title(' 1/Rl5 vs V5');
end
figure; hold on; grid on;
plot(V,Rl*2*Rt,'-'); title(' dimensionless pressure vs Volume');
area1=trapz(V,Rl*2*Rt);                          % area under graph (V,RL)
%% moving bubble(s)

%% assign random values
% matrix mx1 of random numbers picked uniformly between 0 and 1
m=1000;
R=random('unif',1,2,[m 1]);

%% assigning volumes for bubbles
clc;
N=300; %number of bubbles
Vrand=R(unidrnd(m,N,1),1);
Vrand(1,1)=0;
Vrt=zeros(N,1);
for i=1:N-1
    Vrt(i+1,1)=Vrand(i+1)+Vrt(i);
end
Vr=Vrt-fix(Vrt);
Rrand=zeros(N,1);
for i=1:N
    Rrand(i,1)=interp1(V,Rl,Vr(i,1));
end
x=zeros(N,1);
for i=1:N
    x(i,1)=interp1(V,xL,Vr(i,1))*L;
end
Gegevens=[Vrt Vr Rrand x];
disp(Gegevens)
figure; hold on; grid on;
plot(Vrt,Rrand*2*Rt,'o')
figure; hold on; grid on;
plot(Vr,Rrand*2*Rt,'o')
%% incr/decr Vrt
Z=1000;         % amount of iterations   1000;1007;1033;1070;1160;7205
C1=0.0002;      % diffusion rate
0;0.00001;0.00005;0.0001;0.0002;0.0009
C2=0.0001;      % convection rate
area2=zeros(Z,1);
Amzero=zeros(Z,1);
for z=1:Z;
    [Y1,I1] = max(Rl);
    [Y2,I2] = min(Rl);
    for i=1:N
        Gegevens(i,4)=interp1(V,xL,Gegevens(i,2))*L;
% position by new Vrt&Vrand
    end

    for i=1:size(Vrt)-1;
        if Gegevens(i,1)==Gegevens(i+1,1) && Gegevens(i,1)>0;
% total volume is the same as the next total volume, total volume is bigger
than 0;
            disp(i);
            disp('reason: same volumes')
            Gegevens(i,1)=0;
        elseif Gegevens(i,1)+0.05>=Gegevens(i+1,1) && Gegevens(i+1,1)>0;
% 0.05 is just a picked value could be higher/lower or maybe scale with
radius
```

```
            disp(i);
            disp('reason: next volume to close')
            Gegevens(i,1)=0;
        elseif fix(Gegevens(i,1))==fix(Gegevens(i+1,1)) && Gegevens(i,1)>0
&& Gegevens(i+1,3)==0 && Gegevens(i,2)>0 && Gegevens(i,2)<1 &&
Gegevens(i,4)>=Gegevens(i+1,4)-X; % lamella in same pore, total volume
bigger than 0, radius >0, 0<volume in pore<1, position required
            disp(i);
            disp('reason: overlap with rectangle')
            Gegevens(i,1)=0;
        elseif (Rlmax-cosd(t)*Rl0)+(L-x5)/cosd(t)>= L &&
fix(Gegevens(i,1))==fix(Gegevens(i+1,1)) && Gegevens(i,3)>0 &&
Gegevens(i+1,3)<0 && (1/Gegevens(i,3)-cosd(t)*Rl0)+(L-
Gegevens(i+1,4))/cosd(t)>= L;
            disp(i);
            disp('reason: crossing lamella')
            Gegevens(i,1)=0;
        end
    end

    for i=1:N
        if Gegevens(i,1)>0;
            if Gegevens(i,3)<Y1 && Gegevens(i,2)<V(I1);
%1/radius<max(Radius) & V<V at max(radius)
                Gegevens(i,1)=Gegevens(i,1)- C1*(Rl0*Gegevens(i,3))+C2;
            elseif Gegevens(i,3)>Y2 && Gegevens(i,2)>V(I2);
%1/radius>min(Radius) & V>V at min(radius)
                Gegevens(i,1)=Gegevens(i,1)+ C1*abs(Rl0*Gegevens(i,3))+C2;
            elseif Gegevens(i,3)>0;
%1/radius >0
                Gegevens(i,1)=Gegevens(i,1)- C1+C2;
            elseif Gegevens(i,3)< 0;
                Gegevens(i,1)=Gegevens(i,1)+ C1+C2;
%1/radius <0
            else Gegevens(i,1)=Gegevens(i,1)+ C2;
%1/radius=0
            end
        else Gegevens(i,1)=0;
%boudary Vrt(1,1)=0
        end
    end

    Gegevens(:,2)=Gegevens(:,1)-fix(Gegevens(:,1));
    for i=1:N
        Gegevens(i,3)=interp1(V,Rl,Gegevens(i,2));
%Rrand bij nieuwe Vrt&Vrand
    end

    Gegevens=sortrows(Gegevens);
    Amzero(z,1)=find(Gegevens(:,1)==0, 1, 'last' );
% amount of zeros in cumulative volume;
    area2(z,1)=sum(Gegevens(:,3))/(N-Amzero(z,1));
% sum Rrand over amount of non-merged bubbels
    if C1>0 && C2==0 && z>1 && abs(area2(z,1))>0 && abs(area2(z-1,1)) >
abs(area2(z,1)) && abs(area2(z-1,1)) <= abs(area2(z,1))+0.001
        C1=C1*0.75;
        disp(z)
        disp('diffusion decreases')
    end
end
% disp(mean(area2*2*Rt))
```

```
z=1:Z;
figure; hold on; grid on; xlabel('number of iteration'); ylabel('amount
bubbels merged');
plot(z,Amzero,'x')
figure; hold on; grid on; xlabel('iteration step'); ylabel('average Pd');
title('progression line dimensionless pressure');
plot(z,area2*2*Rt,'-')

%% mean vs diffusion/convection

mean=[0.2165;0.2183;0.2282;0.2394;0.2609;0.3978];
diffusion=[0;0.00001;0.00005;0.0001;0.0002;0.0009];
convection=0.001;
figure; hold on; grid on; xlabel('diffusion rate/ convection rate');
ylabel('mean'); title('mean vs (diffusion rate/convection rate)');
plot(diffusion/convection,mean,'o')

% mean=[1737;1803;2062;2379;2988;6845];
```